

Efficient Group Lasso Regularized Rank Regression with Data-Driven Parameter Determination

Meixia Lin* Meijiao Shi† Yunhai Xiao‡ Qian Zhang§

October 14, 2025

Abstract

High-dimensional regression often suffers from heavy-tailed noise and outliers, which can severely undermine the reliability of least-squares based methods. To improve robustness, we adopt a non-smooth Wilcoxon score based rank objective and incorporate structured group sparsity regularization, a natural generalization of the lasso, yielding a group lasso regularized rank regression method. By extending the tuning-free parameter selection scheme originally developed for the lasso, we introduce a data-driven, simulation-based tuning rule and further establish a finite-sample error bound for the resulting estimator. On the computational side, we develop a proximal augmented Lagrangian method for solving the associated optimization problem, which eliminates the singularity issues encountered in existing methods, thereby enabling efficient semismooth Newton updates for the subproblems. Extensive numerical experiments demonstrate the robustness and effectiveness of our proposed estimator against alternatives, and showcase the scalability of the algorithm across both simulated and real-data settings.

keywords: Rank-based regression; Group lasso regularization; Data-driven parameter determination; Proximal augmented Lagrangian method;

1 Introduction

Consider the standard linear model

$$y = X\beta^* + \epsilon, \quad (1)$$

where $y \in \mathbb{R}^n$ is the response vector, $X \in \mathbb{R}^{n \times p}$ is the design matrix, $\beta^* \in \mathbb{R}^p$ is the true coefficient vector, and $\epsilon \in \mathbb{R}^n$ denotes the random errors. Ordinary least squares is the classical approach for estimating β^* and works well under light-tailed noise such as Gaussian errors. However, its reliance on the squared loss makes it highly sensitive to heavy-tailed errors and outliers: a single extreme value can dominate the loss function, leading to highly unstable estimates and compromised predictive performance. Heavy-tailed errors are common in modern high-dimensional data, for

*Engineering Systems and Design, Singapore University of Technology and Design, Singapore (meixia.lin@sutd.edu.sg).

†School of Mathematics and Statistics, Henan University, Zhengzhou 450046, P.R. China (smj@henu.edu.cn)

‡(Corresponding author) School of Mathematics and Statistics & Center for Applied Mathematics of Henan Province, Henan University, Zhengzhou 450046, P.R. China(yhxiao@henu.edu.cn)

§Engineering Systems and Design, Singapore University of Technology and Design, Singapore (qian_zhang@sutd.edu.sg).

example in genomics [Wang et al., 2015] and neuroimaging [Eklund et al., 2016], underscoring the need for robust regression methods that remain reliable in such settings.

To address this issue, a variety of robust estimation techniques have been developed. One prominent line of research employs robust loss functions, which mainly rely on truncation and down-weighting strategies. The Huber estimator [Huber, 1973, Sun et al., 2020] is a classic truncation-based method, which clips gradients beyond a certain threshold to enforce linear growth, thereby diminishing the influence of outliers. Tukey’s biweight estimation [Beaton and Tukey, 1974, Huber, 2011] exemplifies the downweighting approach by employing a bisquare function that gradually reduces the weights of large residuals to zero. While these methods effectively mitigate the impact of outliers via gradient modification, they suffer from an identifiability issue: the global minimizers of the modified losses may not coincide with the true parameter vector [Fan et al., 2016]. An alternative direction is quantile regression [Koenker and Bassett, 1978, Koenker, 2005], which replaces the squared loss with an asymmetric linear loss to directly estimate conditional quantiles, thereby providing robustness against heavy-tailed noise. However, its efficiency is reduced when the specified quantile lies in a sparse region, making extreme quantile estimation particularly challenging. To overcome this limitation, rank-based methods [Hettmansperger and McKean, 2010] reformulate estimation in terms of rank-induced functionals, such as Jaeckel’s dispersion measure [Jaeckel, 1972], to stabilize estimation at sparse quantiles. In particular, Wilcoxon score based rank estimators achieve strong consistency and asymptotic normality, with variance depending only on the rank-transformed error distribution, thereby ensuring robustness against general heavy-tailed noise. The Wilcoxon score based rank estimator corresponds to minimizing the rank loss:

$$L(X\beta - y) := \frac{1}{n(n-1)} \sum_{i=1}^n \sum_{j \neq i} |(X\beta - y)_i - (X\beta - y)_j|. \quad (2)$$

The pairwise differencing structure eliminates the intercept, which makes the estimator invariant to location shifts in ϵ_i , so that no explicit centering assumption on the error distribution is needed. Moreover, when the errors are independent and identically distributed, the distribution of $\epsilon_i - \epsilon_j$ is symmetric about zero, so the expected loss $E(|\epsilon_i - \epsilon_j - (X_i - X_j)^\top(\beta - \beta^*)|)$ is minimized at $\beta = \beta^*$. Replacing the expectation by its empirical counterpart yields (2). Thus minimizing (2) provides a principled sample analogue whose minimizer consistently estimates β^* .

In high-dimensional settings, imposing additional regularization on (2) is essential for variable selection and for incorporating prior structural knowledge among coefficients. Wang et al. [2020] investigated the lasso-regularized estimator based on the rank loss function, introducing a simulation-based parameter determination rule that adapts to both the unknown random error distribution and the structure of the design matrix. Although the lasso penalty effectively induces sparsity in the coefficients, it fails to encode structural constraints such as group sparsity. This capability is critical in a wide range of applications, from biomedical imaging [Janjušević et al., 2025] to deep learning [Lu et al., 2025].

To overcome this limitation, we propose a group lasso regularized rank regression estimator that incorporates the group lasso penalty [Yuan and Lin, 2006] to induce group-level sparsity:

$$\hat{\beta} = \arg \min_{\beta \in \mathbb{R}^p} \{L(X\beta - y) + \lambda \Psi(\beta)\}, \quad (3)$$

where the group lasso regularizer $\Psi : \mathbb{R}^p \rightarrow \mathbb{R}$ is defined as

$$\Psi(\beta) = \sum_{l=1}^g w_l \|\beta_{\mathcal{G}_l}\|_2.$$

Here, $\{\mathcal{G}_l\}_{l=1}^g$ constitutes a partition of the coefficient index set $[p] := \{1, \dots, p\}$ into g predefined, non-overlapping groups, with each group \mathcal{G}_l assigned a positive weight $w_l > 0$. The notation $\beta_{\mathcal{G}_l}$ denotes the subvector of β corresponding to the indices in \mathcal{G}_l . The regularization parameter $\lambda > 0$ controls the trade-off between the goodness-of-fit and the group-wise sparsity. Building on the simulation-based parameter rule proposed by [Wang et al. \[2020\]](#), we extend the framework from the lasso to the group lasso setting, yielding a fully data-driven formula of λ that directly accounts for group structure and avoids the need for computationally intensive cross-validation. Furthermore, we establish a finite-sample error bound for the resulting estimator under mild error assumptions, demonstrating validity even in the presence of heavy-tailed errors commonly observed in high-dimensional data.

To make the proposed estimator (3) practically useful, it is essential to design an efficient algorithm for solving the involved optimization problem. Existing progress on the regularized rank regression problems is rather limited. For the lasso regularized rank regression, [Wang et al. \[2020\]](#) reformulated the rank loss into a linear program with $\mathcal{O}(n^2)$ constraints by introducing slack variables, and then solved it by generic LP solvers. While conceptually straightforward, this approach suffers from poor scalability as the sample size n grows. A more recent advance is the Proximal–Proximal Majorization–Minimization (PPMM) algorithm [\[Tang et al., 2023\]](#), originally developed for rank regression with difference-of-convex penalties, where Algorithm 3 (Step 1) provides an approach for solving rank regression with convex regularization. The method is implemented through a nested triple-loop scheme: an outer proximal point iteration, a middle proximal point loop applied to the dual of each subproblem, and an inner semismooth Newton iteration. This complicated structure arises from the singularity of the generalized Hessian in the dual formulation of the outer subproblem, which prevents the direct application of Newton-type methods. While PPMM achieves reasonable numerical performance, the computational overhead associated with three nested loops limits its scalability in high-dimensional problems.

Motivated by these limitations, our goal is to design an efficient solver that addresses the regularized rank regression problem, with the group lasso regularized case (3) being a notable example, preserving the fast linear convergence properties of proximal point algorithms (or, equivalently, dual augmented Lagrangian methods) without the complexity of such a heavy triple-loop design. To this end, we develop a proximal augmented Lagrangian method (PALM) for solving the dual of (3), equipped with a semismooth Newton (SSN) solver for the resulting subproblems. By augmenting the dual with a proximal term, PALM regularizes the subproblems and eliminates the singularity issue, enabling effective SSN updates which can fully exploit second-order sparsity for rapid local convergence. This yields a framework that retains the desirable convergence behavior of proximal point type methods while avoiding the complexity of PPMM. In addition, unlike subsampling or resampling strategies such as the incomplete U-statistic approach [\[Wang et al., 2020, Fan et al., 2020\]](#), we reformulate the rank loss term as a weighted ordered lasso, which reduces the per-iteration complexity from $\mathcal{O}(n^2)$ to $\mathcal{O}(n \log n)$ and simultaneously facilitates efficient computation of the proximal mapping and the generalized Hessian. Together, these contributions yield a practical and theoretically grounded solver for high-dimensional regularized rank regression with structured sparsity.

The remainder of this paper is organized as follows. In Section 2, we introduce a data-driven simulation-based strategy for determining the regularization parameter λ in the group lasso regularized rank regression model (3), and establish a finite-sample error bound for the resulting estimator. In Section 3, we develop an efficient inexact PALM algorithmic framework applied to the dual of Problem (3), together with implementation details. Comprehensive numerical experiments are presented in Section 4, evaluating both the statistical performance of the proposed estimator, and the computational efficiency of PALM against state-of-the-art solvers. Finally, we conclude our work in Section 5.

Notation. For a positive integer m , let $[m] = \{1, \dots, m\}$. Given a vector $\beta \in \mathbb{R}^p$ and an index set $\mathcal{I} \subseteq [p]$, we denote by $\beta_{\mathcal{I}}$ the subvector indexed by \mathcal{I} , by $\bar{\mathcal{I}}$ its complement, and by $|\mathcal{I}|$ its cardinality. The Euclidean norm is denoted by $\|\cdot\|_2$, while for a positive definite matrix M , the weighted norm is $\|x\|_M := \sqrt{x^T M x}$ with the associated point-to-set distance $\text{dist}_M(x, S) := \inf_{y \in S} \|x - y\|_M$. Let $e_p \in \mathbb{R}^p$ be the vector of all ones, and $\text{sign}(\cdot)$ denote the element-wise sign function: for any scalar t , $\text{sign}(t) = 1$ if $t > 0$, 0 if $t = 0$, and -1 if $t < 0$. Closed balls of radius $r > 0$ in \mathbb{R}^p under the ℓ_1 , ℓ_2 , and ℓ_∞ norms are denoted by \mathcal{B}_1^r , \mathcal{B}_2^r , and \mathcal{B}_∞^r , respectively.

The *Moreau envelope* of a proper, closed, and convex function $f : \mathbb{R}^n \rightarrow \mathbb{R} \cup \{+\infty\}$ with parameter $\sigma > 0$ is defined by

$$e_\sigma f(x) := \min_{y \in \mathbb{R}^n} \left\{ f(y) + \frac{1}{2\sigma} \|y - x\|_2^2 \right\}, \quad x \in \mathbb{R}^n. \quad (4)$$

Following Moreau [1965], the Moreau envelope is continuously differentiable with gradient $\nabla e_\sigma f(x) = (x - \text{Prox}_{\sigma f}(x))/\sigma$, where the proximal operator $\text{Prox}_{\sigma f}(x)$ is the unique minimizer of (4) and is nonexpansive (1-Lipschitz) [Nocedal and Wright, 2006, Rockafellar, 1976a].

2 Data-Driven Regularization with Theoretical Guarantees

2.1 Simulation-Based Parameter

We propose a data-driven method to select the regularization parameter λ for the group lasso regularized rank regression model (3). This approach extends the method of Wang et al. [2020] from the lasso to the group lasso setting, accommodating structured sparsity.

For any $\beta \in \mathbb{R}^p$, define the estimation error $\gamma := \beta - \beta^*$. From (1), we have

$$X\beta - y = X(\beta - \beta^*) - \epsilon = X\gamma - \epsilon.$$

Consequently, minimizing the objective in (3) is equivalent to solving

$$\min_{\gamma \in \mathbb{R}^p} \{F_\lambda(\gamma) := L_0(\gamma) + \lambda \Psi(\gamma + \beta^*)\}, \quad (5)$$

where the shifted loss function $L_0 : \mathbb{R}^p \rightarrow \mathbb{R}$ is defined as

$$L_0(\gamma) := \frac{1}{n(n-1)} \sum_{i=1}^n \sum_{j \neq i} |(\epsilon_i - \epsilon_j) - (X_i - X_j)^T \gamma|. \quad (6)$$

This reformulation plays a central role in deriving both the simulation-based parameter determination rule and the corresponding finite-sample error bound.

Let S_n denote the subgradient of $L_0(\cdot)$ evaluated at $\gamma = 0$. The following result, adapted from Wang et al. [2020, Lemma 1], characterizes the distribution of the random vector S_n , which is shown to be independent of the error distribution.

Lemma 1. *Under the linear model (1), the subgradient of $L_0(\cdot)$ in (6) at $\gamma = 0$ is*

$$S_n = -\frac{2}{n(n-1)} X^\top \xi, \quad (7)$$

where $\xi = 2r - (n+1)$ and r is uniformly distributed over all permutations of $[n]$.

Motivated by this completely pivotal property of S_n , we propose the following fully data-driven choice of regularization parameter for the problem (3):

$$\lambda^* = c_0 \cdot Q_{\Psi^d(S_n)}(1 - \alpha_0), \quad (8)$$

where $c_0 > 1$ and $0 < \alpha_0 < 1$ are user-specified constants, and $Q_{\Psi^d(S_n)}(1 - \alpha_0)$ is the $(1 - \alpha_0)$ -quantile of the random variable $\Psi^d(S_n)$. Here,

$$\Psi^d(y) := \sup_{\Psi(x) \leq 1} \langle x, y \rangle = \max_{1 \leq l \leq g} \frac{\|y_{\mathcal{G}_l}\|_2}{w_l} \quad (9)$$

is the dual norm of $\Psi(\cdot)$. Notably, the proposed λ^* in (8) does not rely on any assumptions about the error distribution, as guaranteed by Lemma 1. In practice, we can compute λ^* via Monte Carlo simulation, see Algorithm 1.

Algorithm 1 Simulation-based choice of regularization parameter λ

Input: Design matrix $X \in \mathbb{R}^{n \times p}$, predefined groups $\{\mathcal{G}_l\}_{l=1}^g$ with weights $\{w_l\}_{l=1}^g$, quantile level $0 < \alpha_0 < 1$, scale factor $c_0 > 1$, simulation number $K (= 500)$

- 1: **for** $k = 1$ to K **do**
- 2: Generate a random permutation $r^{(k)}$ of $[n]$ and compute $\xi^{(k)} = 2r^{(k)} - (n+1)$
- 3: Compute subgradient $S_n^{(k)} = -\frac{2}{n(n-1)} X^\top \xi^{(k)}$.
- 4: Evaluate $\Psi^d(S_n^{(k)}) = \max_{1 \leq l \leq g} \left(\|(S_n^{(k)})_{\mathcal{G}_l}\|_2 / w_l \right)$.
- 5: **end for**

Output: $\lambda^* = c_0 \cdot q_{1-\alpha_0}$, where $q_{1-\alpha_0}$ be the empirical $(1 - \alpha_0)$ -quantile of $\{\Psi^d(S_n^{(k)})\}_{k=1}^K$.

Remark 1. *In Algorithm 1, the constant c_0 serves as a safety factor for the regularization parameter, whereas α_0 specifies the confidence level for the error bound established in the next subsection. Their roles will be further clarified in Theorem 1. In practice, values such as $c_0 = 1.01$ and $\alpha_0 = 0.1$ are simple and effective choices.*

2.2 Finite-Sample Bound on Estimation Error

Building upon the data-driven parameter selection, we now establish a finite-sample bound on the estimation error of the resulting estimator. To facilitate the analysis, we introduce the following notations. Let $\mathcal{S}_0 := \{j \in [p] : (\beta^*)_j \neq 0\}$ denote the support of the true parameter β^* , with

cardinality $q = |\mathcal{S}_0|$. Define the set of active group indices and the associated group-expanded support as

$$\mathcal{A}_0 := \{l \in [g] : \mathcal{G}_l \cap \mathcal{S}_0 \neq \emptyset\} \quad \text{and} \quad \Omega := \bigcup_{l \in \mathcal{A}_0} \mathcal{G}_l.$$

Next, we consider the regularizer $\Psi(\cdot)$ defined in (3), and define its restriction to Ω as

$$\Psi_\Omega(\beta) := \Psi(\mathcal{P}_\Omega(\beta)), \quad \beta \in \mathbb{R}^p,$$

where $\mathcal{P}_\Omega(\beta)$ denotes the projection of β onto Ω , that is, a vector in \mathbb{R}^p that agrees with β on the coordinates in Ω and is zero elsewhere. Similarly, we define $\Psi_{\bar{\Omega}}(\beta) := \Psi(\mathcal{P}_{\bar{\Omega}}(\beta))$, where $\bar{\Omega} := [p] \setminus \Omega$ denotes the complement of Ω . This decomposition gives rise to the following key properties, which are essential for the finite-sample error analysis. For any $\beta \in \mathbb{R}^p$, we have

$$\Psi(\beta) = \Psi_\Omega(\beta) + \Psi_{\bar{\Omega}}(\beta), \quad (10)$$

$$\Psi_\Omega(\beta) \leq c_{|\Omega|} \|\beta\|_2, \quad \text{with} \quad c_{|\Omega|} = \sqrt{\sum_{l \in \mathcal{A}_0} w_l^2}, \quad (11)$$

$$\Psi^d(\beta) \leq c_p \|\beta\|_\infty, \quad \text{with} \quad c_p = \max_{1 \leq l \leq g} w_l^{-1} \sqrt{|\mathcal{G}_l|}, \quad (12)$$

where $\Psi^d(\cdot)$ denotes the dual norm associated with $\Psi(\cdot)$, as defined in (9).

To establish finite-sample guarantees for our estimator, we impose the following technical conditions on the design matrix and error distribution.

Assumption 1. *We impose the following assumptions to ensure the error bound guarantee.*

(A-1) **Design Matrix Condition.** *The covariates are empirically centered, i.e., $\sum_{i=1}^n X_i = 0$, and uniformly bounded by a constant $b_1 > 0$, i.e., $|X_{ij}| \leq b_1$ for all i, j . Furthermore, the design matrix satisfies the restricted eigenvalue (RE) condition*

$$\inf_{\gamma \in \mathbb{R}^p} \left\{ \frac{\gamma^\top X^\top X \gamma}{n \|\gamma\|_2^2} : \Psi_{\bar{\Omega}}(\gamma) \leq (\bar{c} - 1) \Psi_\Omega(\gamma) \right\} \geq b_2,$$

where $b_2 > 0$ is a constant and $\bar{c} := 1 + \frac{c_0+1}{c_0-1}$, with c_0 the user-specified constant in (8).

(A-2) **Error Distribution Condition.** *The random errors ϵ_i are i.i.d. with density function $f(\cdot)$. Let $\zeta_{ij} := \epsilon_i - \epsilon_j$ for $i \neq j$, and denote by $F^*(\cdot)$ and $f^*(\cdot)$ cumulative distribution function and probability density function of ζ_{ij} , respectively. There exists a constant $b_3 > 0$ such that, for all i, j ,*

$$f^*(\zeta_{ij}) \geq b_3 \quad \text{uniformly for all } |\zeta_{ij}| \leq \frac{68b_1^2 c_0 \bar{c}^2}{b_2 b_3} c_p^2 c_{|\Omega|}^2 \mathcal{E}(n, p).$$

Here $\mathcal{E}(n, p) := n^{-1} \log p + \sqrt{n^{-1} \log p}$, and the constants c_p and $c_{|\Omega|}$ are defined in (12) and (11), respectively.

For better understanding, we give the following discussions on the above assumptions.

Remark 2. Assumption 1 is in line with conditions commonly imposed in high-dimensional regression with rank-based methods. The RE condition on the design matrix is standard in the analysis of ℓ_1 -type regularization [Bickel et al., 2009, Negahban et al., 2012]. For the error distribution, it is typical to assume i.i.d. errors with a continuous density bounded away from zero near the origin, as in the analysis of Wilcoxon-type estimators [Jurečková and Sen, 1996, Wang et al., 2020]. In the following, we clarify their roles and discuss common scenarios in which they are typically satisfied.

- (a1) Assumption (A-1) imposes a RE condition over a structured cone based on the decomposition of the regularizer $\Psi(\cdot)$ across the active and inactive groups. The choice of parameter in (8) guarantees that the estimation error $\hat{\gamma}(\lambda^*) := \hat{\beta}(\lambda^*) - \beta^*$ lies in this cone with probability $1 - \alpha_0$ (see Lemma 2).
- (a2) Assumption (A-2) requires the pairwise error difference density $f^*(\cdot)$ to be bounded away from zero near the origin. Let $K := (68b_1^2c_0\bar{c}^2/b_2)c_p^2c_{|\Omega|}^2\mathcal{E}(n, p)$, then Assumption (A-2) is equivalent to requiring the existence of some $M > 0$ such that

$$Mf^*(\zeta) \geq K \quad \text{for all } |\zeta| \leq M. \quad (13)$$

This condition holds for many common error distributions. For example, if the error is unimodal, such as Gaussian, Cauchy, Student's t , and $\chi^2(k)$ with $k \geq 1$, then $f^*(\cdot)$ is symmetric about zero, non-decreasing on $(-\infty, 0]$ and non-increasing on $[0, \infty)$, see Purkayastha [1998, Theorem 2.2]. Consequently, the infimum of $\zeta \mapsto Mf^*(\zeta)$ over $[-M, M]$ is attained at $|\zeta| = M$, so condition (13) simplifies to

$$Mf^*(M) \geq K,$$

in which case such an M exists as long as K is sufficiently small.

We are now ready to provide a finite-sample bound on the estimation error of the proposed group lasso regularized rank regression estimator (3) with the simulation-based parameter (8). The proof is detailed in Section 2.3.

Theorem 1. Suppose Assumption 1 hold. If $p \geq 2/\alpha_0$, then the group lasso regularized rank regression estimator $\hat{\beta}(\lambda^*)$ defined in (3), with the regularization parameter λ^* specified in (8), satisfies

$$\|\hat{\beta}(\lambda^*) - \beta^*\|_2 \leq \frac{34b_1c_0\bar{c}}{b_2b_3}c_{|\Omega|}c_p\mathcal{E}(n, p)$$

with probability at least $1 - \exp(-n\mathcal{E}^2(n, p)) - \alpha_0$. Here, the constants $c_{|\Omega|}$ and c_p are defined in (11) and (12), respectively; the constants c_0 and α_0 are given in (8); and the constants \bar{c} , b_1 , b_2 , and b_3 are specified in Assumption 1.

In particular, when $\log p \ll n$ and the group lasso weights are chosen as $w_l = |\mathcal{G}_l|^{-1/2}$, the error bound in the above theorem simplifies to a more interpretable form, stated as the following corollary.

Corollary 1. Suppose Assumption 1 hold. If $e^n \gg p \geq 2/\alpha_0$, then the group lasso regularized rank regression estimator $\hat{\beta}(\lambda^*)$ defined in (3) with the regularization parameter λ^* from (8) and weights $w_l = |\mathcal{G}_l|^{-1/2}$, satisfies

$$\|\hat{\beta}(\lambda^*) - \beta^*\|_2 \leq \frac{68b_1c_0\bar{c}}{b_2b_3}\sqrt{\frac{|\Omega|\log p}{n}},$$

with probability at least $1 - p^{-1} - \alpha_0$.

Note that Theorem 1 recovers the results for the following estimators as special cases.

- (1) *Lasso*: $\Psi(\beta) = \|\beta\|_1$, where each group consists of a single coordinate. In this case, $c_{|\Omega|} = \sqrt{q}$, $c_p = 1$, and Corollary 1 yields an error bound that is essentially equivalent to the known rate for the rank lasso estimator established in Wang et al. [2020].
- (2) *Weighted lasso*: $\Psi(\beta) = \sum_{j=1}^p w_j |\beta_j|$ with $w_j > 0$, $j \in [p]$. In particular, if $w_j = \mathcal{O}(1)$ uniformly, Theorem 1 yields the bound $\|\hat{\beta}(\lambda^*) - \beta^*\|_2 \lesssim \sqrt{q \log p/n}$ under the condition $\log p \ll n$.

Beyond these, our general result in Theorem 1 extends beyond the group lasso setting and applies to any regularizer $\Psi(\cdot)$ satisfying the following three properties: (i) subadditivity (i.e., the triangle inequality) $\Psi(\alpha + \beta) \leq \Psi(\alpha) + \Psi(\beta)$; (ii) support decomposability as formalized in (10); and (iii) norm compatibility as required in (11) and (12), without assuming a specific form of the associated constants. We omit the proof here, as it follows directly from a straightforward modification of our main argument in Section 2.3.

2.3 Proof of Theorem 1

This subsection presents the proof of Theorem 1, which establishes a finite-sample error bound for the proposed estimator (3) under the simulation-based regularization parameter (8). The argument relies on two key probabilistic ingredients, each stated as a supporting lemma, with proofs in Appendix A. The first lemma ensures that the estimation error lies within a structured cone with high probability as follows.

Lemma 2. *For the group lasso regularized rank regression estimator $\hat{\beta}(\lambda^*)$ in (3) with the regularization parameter λ^* specified in (8), the estimation error $\hat{\gamma}(\lambda^*) := \hat{\beta}(\lambda^*) - \beta^*$ satisfies*

$$\text{pr} \left(\Psi_{\bar{\Omega}}(\hat{\gamma}(\lambda^*)) \leq \frac{c_0 + 1}{c_0 - 1} \Psi_{\Omega}(\hat{\gamma}(\lambda^*)) \right) = 1 - \alpha_0.$$

The second lemma provides a high-probability tail bound for the dual norm $\Psi^d(\cdot)$ at the empirical gradient S_n in (7), which helps justify the proposed regularization parameter.

Lemma 3. *Suppose Assumption (A-1) holds. Then for any $t > 0$,*

$$\text{pr} \left(\Psi^d(S_n) \geq t \right) \leq 2p \exp \left(-\frac{nt^2}{32b_1^2 c_p^2} \right).$$

We then give the proof of the main theorem as follows.

of Theorem 1. Define the sets

$$\Gamma = \{\gamma \in \mathbb{R}^p : \Psi_{\bar{\Omega}}(\gamma) \leq (\bar{c} - 1)\Psi_{\Omega}(\gamma)\} \text{ and } \Gamma^* = \{\gamma \in \Gamma : \|\gamma\|_2 = \Delta c_{|\Omega|} c_p \mathcal{E}(n, p)\},$$

where $\Delta = \frac{34b_1 c_0 \bar{c}}{b_2 b_3}$. Define the estimation error $\hat{\gamma}(\lambda^*) := \hat{\beta}(\lambda^*) - \beta^*$. Then we have that

$$\text{pr} \left(\|\hat{\beta}(\lambda^*) - \beta^*\|_2 \leq \Delta c_{|\Omega|} c_p \mathcal{E}(n, p) \right) = 1 - \text{pr} \left(\|\hat{\gamma}(\lambda^*)\|_2 > \Delta c_{|\Omega|} c_p \mathcal{E}(n, p) \right)$$

$$\begin{aligned}
&\geq 1 - \text{pr}(\{\|\hat{\gamma}(\lambda^*)\|_2 > \Delta c_{|\Omega|} c_p \mathcal{E}(n, p)\} \cap \{\hat{\gamma}(\lambda^*) \in \Gamma\}) - \text{pr}(\hat{\gamma}(\lambda^*) \notin \Gamma) \\
&\geq 1 - \text{pr}\left(\inf_{\gamma \in \Gamma} \{F_{\lambda^*}(\gamma) \mid \|\gamma\|_2 > \Delta c_{|\Omega|} c_p \mathcal{E}(n, p)\} \leq F_{\lambda^*}(0)\right) - \text{pr}(\hat{\gamma}(\lambda^*) \notin \Gamma),
\end{aligned}$$

where $F_\lambda(\cdot)$ is defined in (5), and the last inequality follows from the fact that when $\|\hat{\gamma}(\lambda^*)\|_2 > \Delta c_{|\Omega|} c_p \mathcal{E}(n, p)$ and $\hat{\gamma}(\lambda^*) \in \Gamma$, we have

$$\inf_{\gamma \in \Gamma} \{F_{\lambda^*}(\gamma) \mid \|\gamma\|_2 > \Delta c_{|\Omega|} c_p \mathcal{E}(n, p)\} = F_{\lambda^*}(\hat{\gamma}(\lambda^*)) = \inf_{\gamma \in \mathbb{R}^p} F_{\lambda^*}(\gamma) \leq F_{\lambda^*}(0).$$

Moreover, we can see that

$$\begin{aligned}
&\text{pr}\left(\|\hat{\beta}(\lambda^*) - \beta^*\|_2 \leq \Delta c_{|\Omega|} c_p \mathcal{E}(n, p)\right) \\
&\geq \text{pr}\left(\inf_{\gamma \in \Gamma} \{F_{\lambda^*}(\gamma) \mid \|\gamma\|_2 > \Delta c_{|\Omega|} c_p \mathcal{E}(n, p)\} > F_{\lambda^*}(0)\right) - \alpha_0 \geq \text{pr}\left(\inf_{\gamma \in \Gamma^*} F_{\lambda^*}(\gamma) > F_{\lambda^*}(0)\right) - \alpha_0,
\end{aligned} \tag{14}$$

where the first inequality comes from Lemma 2, and the second inequality follows from Lemma 4 in Appendix A. Denote $E(L_0(\cdot))$ as $\bar{L}_0(\cdot)$, where $L_0(\cdot)$ is defined in (6). By the definition of $F_\lambda(\cdot)$ in (5) and the triangle inequality, we have

$$\begin{aligned}
\inf_{\gamma \in \Gamma^*} \{F_{\lambda^*}(\gamma) - F_{\lambda^*}(0)\} &= \inf_{\gamma \in \Gamma^*} \{L_0(\gamma) + \lambda^* \Psi(\gamma + \beta^*) - L_0(0) - \lambda^* \Psi(\beta^*)\} \\
&= \inf_{\gamma \in \Gamma^*} \{\bar{L}_0(\gamma) - \bar{L}_0(0) + L_0(\gamma) - L_0(0) - (\bar{L}_0(\gamma) - \bar{L}_0(0)) + \lambda^* (\Psi(\gamma + \beta^*) - \Psi(\beta^*))\} \\
&\geq \underbrace{\inf_{\gamma \in \Gamma^*} \{\bar{L}_0(\gamma) - \bar{L}_0(0)\}}_{\text{part I}} - \underbrace{\eta(\Gamma^*)}_{\text{part II}} - \underbrace{\lambda^* \sup_{\gamma \in \Gamma^*} |\Psi(\gamma + \beta^*) - \Psi(\beta^*)|}_{\text{part III}},
\end{aligned} \tag{15}$$

where $\eta(\Gamma^*) := \sup_{\gamma \in \Gamma^*} |L_0(\gamma) - L_0(0) - (\bar{L}_0(\gamma) - \bar{L}_0(0))|$.

Next, we analyze the bounds for three parts one by one. To facilitate the subsequent analysis, for any $\gamma \in \Gamma$, we define an auxiliary function $h_\gamma : \mathbb{R}^2 \rightarrow \mathbb{R}$ as:

$$h_\gamma(\epsilon_i, \epsilon_j) := |(\epsilon_i - \epsilon_j) - (X_i - X_j)^\top \gamma| - |\epsilon_i - \epsilon_j|.$$

Then we can see that, for each $i, j \in [p]$,

$$|h_\gamma(\epsilon_i, \epsilon_j)| \leq |(X_i - X_j)^\top \gamma| \leq |\Psi^d(X_i - X_j) \Psi(\gamma)| \leq c_p \|X_i - X_j\|_\infty \Psi(\gamma), \tag{16}$$

where the last inequality follows from (12). For any $\gamma \in \Gamma$, due to decomposition (10) and inequality (11), we have

$$\Psi(\gamma) = \Psi_\Omega(\gamma) + \Psi_{\bar{\Omega}}(\gamma) \leq \bar{c} \Psi_\Omega(\gamma) \leq \bar{c} c_{|\Omega|} \|\gamma\|_2. \tag{17}$$

This, together with (16) and Assumption 1, further implies

$$|h_\gamma(\epsilon_i, \epsilon_j)| \leq 2b_1 \bar{c} c_{|\Omega|} c_p \|\gamma\|_2. \tag{18}$$

Bound for $\inf_{\gamma \in \Gamma^*} \{\bar{L}_0(\gamma) - \bar{L}_0(0)\}$ in part I. By the definition of $\bar{L}_0(\cdot)$, for any $\gamma \in \Gamma^*$, we have

$$\bar{L}_0(\gamma) - \bar{L}_0(0) = E \left(\frac{1}{n(n-1)} \sum_{i=1}^n \sum_{j \neq i} h_\gamma(\epsilon_i, \epsilon_j) \right).$$

According to Knight's identity [Koenker, 2005], it can be seen that

$$h_\gamma(\epsilon_i, \epsilon_j) = -(X_i - X_j)^\top \gamma \left[\frac{1}{2} - \mathbf{1}(\zeta_{ij} < 0) \right] + \int_0^{(X_i - X_j)^\top \gamma} [\mathbf{1}(\zeta_{ij} \leq s) - \mathbf{1}(\zeta_{ij} \leq 0)] ds,$$

where $\zeta_{ij} = \epsilon_i - \epsilon_j$, and $\mathbf{1}(\cdot)$ denotes the indicator function, which equals 1 if the condition inside the braces holds, and 0 otherwise. Since ϵ_i 's are i.i.d., the random variable ζ_{ij} follows a symmetric distribution with cumulative distribution function $F^*(\cdot)$, implying that $E(\mathbf{1}(\zeta_{ij} \leq 0)) = 0.5$. Thus, we can see that for any $\gamma \in \Gamma^*$,

$$\begin{aligned} \bar{L}_0(\gamma) - \bar{L}_0(0) &= \frac{1}{n(n-1)} \sum_{i=1}^n \sum_{j \neq i} \int_0^{(X_i - X_j)^\top \gamma} [F^*(s) - F^*(0)] ds \\ &= \frac{1}{n(n-1)} \sum_{i=1}^n \sum_{j \neq i} \int_0^{(X_i - X_j)^\top \gamma} [F^*(s) - F^*(0)] \mathbf{1}((X_i - X_j)^\top \gamma > 0) ds \\ &\quad + \frac{1}{n(n-1)} \sum_{i=1}^n \sum_{j \neq i} \int_0^{(X_i - X_j)^\top \gamma} [F^*(s) - F^*(0)] \mathbf{1}((X_i - X_j)^\top \gamma \leq 0) ds. \end{aligned}$$

By the Mean Value Theorem, for $\gamma \in \Gamma^*$ with $(X_i - X_j)^\top \gamma > 0$, there exists $\zeta_{ij} \in [0, (X_i - X_j)^\top \gamma]$ such that

$$\int_0^{(X_i - X_j)^\top \gamma} [F^*(s) - F^*(0)] ds = \int_0^{(X_i - X_j)^\top \gamma} s f^*(\zeta_{ij}) ds.$$

From (16) and (18), we know that

$$|\zeta_{ij}| \leq |(X_i - X_j)^\top \gamma| \leq 2b_1 \bar{c} c_{|\Omega|} c_p \|\gamma\|_2 = \frac{68b_1^2 c_0 \bar{c}^2}{b_2 b_3} c_p^2 c_{|\Omega|}^2 \mathcal{E}(n, p).$$

Thus from Assumption (A-2), we know that $f^*(\zeta_{ij}) \geq b_3$, which yields

$$\int_0^{(X_i - X_j)^\top \gamma} [F^*(s) - F^*(0)] ds \geq \frac{b_3}{2} [(X_i - X_j)^\top \gamma]^2.$$

A similar bound holds when $\gamma \in \Gamma^*$ with $(X_i - X_j)^\top \gamma \leq 0$. Therefore, for any $\gamma \in \Gamma^*$, we have

$$\begin{aligned} \bar{L}_0(\gamma) - \bar{L}_0(0) &\geq \frac{b_3}{2n(n-1)} \sum_{i=1}^n \sum_{j \neq i} [(X_i - X_j)^\top \gamma]^2 = \frac{b_3}{2n(n-1)} \sum_{i=1}^n \sum_{j \neq i} \left[(X_i^\top \gamma)^2 + (X_j^\top \gamma)^2 - 2\gamma^\top X_i X_j^\top \gamma \right] \\ &= \frac{b_3}{2n(n-1)} \left(2(n-1) \sum_{i=1}^n (X_i^\top \gamma)^2 - \sum_{i=1}^n \left(\sum_{j \neq i} 2\gamma^\top X_i X_j^\top \gamma + 2\gamma^\top X_i X_i^\top \gamma - 2(X_i^\top \gamma)^2 \right) \right) \\ &= \frac{b_3}{2n(n-1)} \left(2n \sum_{i=1}^n (X_i^\top \gamma)^2 - 2\gamma^\top \left(\sum_{i=1}^n X_i \right) \left(\sum_{j=1}^n X_j \right)^\top \gamma \right) = \frac{b_3}{n-1} \sum_{i=1}^n (X_i^\top \gamma)^2 > \frac{b_3}{n} \sum_{i=1}^n (X_i^\top \gamma)^2, \end{aligned}$$

where the last equality follows from $\sum_{i=1}^n X_i = 0$ in Assumption (A-1). Applying Assumption (A-1) then yields

$$\inf_{\gamma \in \Gamma^*} \{\bar{L}_0(\gamma) - \bar{L}_0(0)\} > \frac{b_3}{n} \inf_{\gamma \in \Gamma^*} \sum_{i=1}^n (X_i^\top \gamma)^2 \geq b_2 b_3 \inf_{\gamma \in \Gamma^*} \|\gamma\|_2^2 = b_2 b_3 \Delta^2 c_{|\Omega|}^2 c_p^2 \mathcal{E}^2(n, p). \quad (19)$$

Bound for $\eta(\Gamma^*)$ in part II. By the bounded difference inequality [McDiarmid, 1989], for any $\delta > 0$, we have

$$\text{pr}(\eta(\Gamma^*) - E(\eta(\Gamma^*)) > \delta) \leq \exp\left(-\frac{2\delta^2}{\sum_{l=1}^n |\eta(\Gamma^*) - \eta^l(\Gamma^*)|^2}\right), \quad (20)$$

where $\eta^l(\Gamma^*)$ is the value of $\eta(\Gamma^*)$ when the l -th observation ϵ_l is replaced by ε_l , with all other observations held fixed. In this case, the loss function $L_0(\cdot)$ is updated to $L_0^l(\cdot)$. For any $\gamma \in \Gamma^*$, the function $h_\gamma(\epsilon_i, \epsilon_j)$ is similarly affected and replaced by $h_\gamma^l(\epsilon_i, \epsilon_j)$, where $h_\gamma^l(\epsilon_i, \epsilon_j) = h_\gamma(\varepsilon_l, \epsilon_j)$ if $i = l$, or $h_\gamma(\epsilon_i, \varepsilon_l)$ if $j = l$; otherwise, it remains unchanged. Then we have that for each $l \in [n]$,

$$\begin{aligned} |\eta(\Gamma^*) - \eta^l(\Gamma^*)| &\leq \sup_{\gamma \in \Gamma^*} \left| L_0(\gamma) - L_0(0) - L_0^l(\gamma) + L_0^l(0) \right| \\ &= \frac{1}{n(n-1)} \sup_{\gamma \in \Gamma^*} \sum_{i=1}^n \sum_{j \neq i} \left| h_\gamma(\epsilon_i, \epsilon_j) - h_\gamma^l(\epsilon_i, \epsilon_j) \right| = \frac{2}{n(n-1)} \sup_{\gamma \in \Gamma^*} \sum_{j \neq l} |h_\gamma(\epsilon_l, \epsilon_j) - h_\gamma(\varepsilon_l, \epsilon_j)| \\ &\leq \frac{2}{n(n-1)} \sup_{\gamma \in \Gamma^*} 4(n-1) b_1 \bar{c} c_{|\Omega|} c_p \|\gamma\|_2 \leq \frac{8b_1 c_0 \bar{c} \Delta}{n} c_{|\Omega|}^2 c_p^2 \mathcal{E}^2(n, p), \end{aligned}$$

where the first inequality follows from the triangle inequality, the second inequality comes from (18), and the last inequality comes from the definition of Γ^* and the fact that $c_0 > 1$. By taking $\delta = 4\sqrt{2}b_1 c_0 \bar{c} \Delta c_{|\Omega|}^2 c_p^2 \mathcal{E}^2(n, p)$ in (20), we obtain

$$\text{pr}\left(\eta(\Gamma^*) - E(\eta(\Gamma^*)) > 4\sqrt{2}b_1 c_0 \bar{c} \Delta c_{|\Omega|}^2 c_p^2 \mathcal{E}^2(n, p)\right) \leq \exp(-n\mathcal{E}^2(n, p)). \quad (21)$$

Then we proceed to bound $E(\eta(\Gamma^*))$. Define M_n to be the smallest integer not less than $n/2$. For any $\gamma \in \Gamma^*$, we can see that

$$L_0(\gamma) - L_0(0) = \frac{1}{n} \sum_{i=1}^n \frac{1}{n-1} \sum_{j \neq i} h_\gamma(\epsilon_i, \epsilon_j) = \frac{1}{n!} \sum_{\pi \in P_n} M_n^{-1} \sum_{i=1}^{M_n} h_\gamma(\epsilon_{\pi(i)}, \epsilon_{\pi(M_n+i)}),$$

where P_n denotes the set of all permutations of $[n]$. It then follows that

$$\begin{aligned} E(\eta(\Gamma)) &= E\left(\sup_{\gamma \in \Gamma^*} \frac{1}{n!} \left| \sum_{\pi \in P_n} M_n^{-1} \sum_{i=1}^{M_n} (h_\gamma(\epsilon_{\pi(i)}, \epsilon_{\pi(M_n+i)}) - E(h_\gamma(\epsilon_{\pi(i)}, \epsilon_{\pi(M_n+i)}))) \right| \right) \\ &= E_\epsilon \left(\sup_{\gamma \in \Gamma^*} \frac{1}{n!} \left| E_{\epsilon'} \left(\sum_{\pi \in P_n} M_n^{-1} \sum_{i=1}^{M_n} (h_\gamma(\epsilon_{\pi(i)}, \epsilon_{\pi(M_n+i)}) - h_\gamma(\epsilon'_{\pi(i)}, \epsilon'_{\pi(M_n+i)})) \right) \right| \right) \\ &\leq \frac{1}{n!} \sum_{\pi \in P_n} E_{\epsilon, \epsilon'} \left(\sup_{\gamma \in \Gamma^*} \left| M_n^{-1} \sum_{i=1}^{M_n} (h_\gamma(\epsilon_{\pi(i)}, \epsilon_{\pi(M_n+i)}) - h_\gamma(\epsilon'_{\pi(i)}, \epsilon'_{\pi(M_n+i)})) \right| \right). \end{aligned}$$

Let $\{\sigma_i\}_{i=1}^n$ be an i.i.d. Rademacher sequence, where each σ_i takes values ± 1 with equal probability. Since the distribution of $h_\gamma(\epsilon_{\pi(i)}, \epsilon_{\pi(M_n+i)}) - h_\gamma(\epsilon'_{\pi(i)}, \epsilon'_{\pi(M_n+i)})$ is symmetric, the random variables

$$\sigma_i \left[h_\gamma(\epsilon_{\pi(i)}, \epsilon_{\pi(M_n+i)}) - h_\gamma(\epsilon'_{\pi(i)}, \epsilon'_{\pi(M_n+i)}) \right] \text{ and } h_\gamma(\epsilon_{\pi(i)}, \epsilon_{\pi(M_n+i)}) - h_\gamma(\epsilon'_{\pi(i)}, \epsilon'_{\pi(M_n+i)})$$

share the same distribution. Therefore,

$$\begin{aligned} E(\eta(\Gamma^*)) &\leq \frac{1}{n!} \sum_{\pi \in P_n} E_{\epsilon, \epsilon', \sigma} \left(\sup_{\gamma \in \Gamma^*} \left| M_n^{-1} \sum_{i=1}^{M_n} \sigma_i (h_\gamma(\epsilon_{\pi(i)}, \epsilon_{\pi(M_n+i)}) - h_\gamma(\epsilon'_{\pi(i)}, \epsilon'_{\pi(M_n+i)})) \right| \right) \\ &\leq \frac{2}{n!} \sum_{\pi \in P_n} E_{\epsilon, \sigma} \left(\sup_{\gamma \in \Gamma^*} \left| M_n^{-1} \sum_{i=1}^{M_n} \sigma_i h_\gamma(\epsilon_{\pi(i)}, \epsilon_{\pi(M_n+i)}) \right| \right), \end{aligned}$$

where the last inequality follows from the triangle inequality. Since $h_\gamma(\epsilon_i, \epsilon_j)$ is a contraction mapping satisfying $|h_\gamma(\epsilon_i, \epsilon_j)| \leq |(X_i - X_j)^\top \gamma|$, an application of the comparison properties for Rademacher averages [Ledoux and Talagrand, 1991, Theorem 4.12] yields

$$\begin{aligned} E(\eta(\Gamma^*)) &\leq \frac{4}{n!} \sum_{\pi \in P_n} E_\sigma \left(\sup_{\gamma \in \Gamma^*} \left| M_n^{-1} \sum_{i=1}^{M_n} \sigma_i (X_{\pi(i)} - X_{\pi(M_n+i)})^\top \gamma \right| \right) \\ &\leq \frac{4}{n!} \sum_{\pi \in P_n} E_\sigma \left(\Psi^d \left(M_n^{-1} \sum_{i=1}^{M_n} \sigma_i (X_{\pi(i)} - X_{\pi(M_n+i)}) \right) \sup_{\gamma \in \Gamma^*} \Psi(\gamma) \right) \\ &\leq \frac{4\bar{c}}{n!} \Delta c_{|\Omega|}^2 c_p^2 \mathcal{E}(n, p) \sum_{\pi \in P_n} E_\sigma \left(\left\| M_n^{-1} \sum_{i=1}^{M_n} \sigma_i (X_{\pi(i)} - X_{\pi(M_n+i)}) \right\|_\infty \right), \end{aligned} \quad (22)$$

where the last inequality follows from (17) and (12). By applying Bühlmann and Van De Geer [2011, Lemma 14.12], we obtain that

$$\begin{aligned} E_\sigma \left(\max_{1 \leq j \leq p} \left| M_n^{-1} \sum_{i=1}^{M_n} \sigma_i (X_{\pi(i),j} - X_{\pi(M_n+i),j}) \right| \right) \\ \leq 2b_1 M_n^{-1} \log(p+1) + \sqrt{2M_n^{-1} \log(p+1)} \leq 5b_1 \left(n^{-1} \log p + \sqrt{n^{-1} \log p} \right) = 5b_1 \mathcal{E}(n, p). \end{aligned}$$

Combining this bound with (22), we have

$$E(\eta(\Gamma^*)) \leq 20b_1 \bar{c} \Delta c_{|\Omega|}^2 c_p^2 \mathcal{E}^2(n, p) \leq 20b_1 c_0 \bar{c} \Delta c_{|\Omega|}^2 c_p^2 \mathcal{E}^2(n, p),$$

which together with (21), implies

$$\text{pr} \left(\eta(\Gamma^*) \leq (20 + 4\sqrt{2})b_1 c_0 \bar{c} \Delta c_{|\Omega|}^2 c_p^2 \mathcal{E}^2(n, p) \right) \geq 1 - \exp(-n\mathcal{E}^2(n, p)). \quad (23)$$

Bound for $\lambda^* \sup_{\gamma \in \Gamma^*} \{|\Psi(\gamma + \beta^*) - \Psi(\beta^*)|\}$ in part III. It can be seen that

$$\lambda^* \sup_{\gamma \in \Gamma^*} \{|\Psi(\gamma + \beta^*) - \Psi(\beta^*)|\} \leq \lambda^* \sup_{\gamma \in \Gamma^*} \Psi(\gamma) \leq \lambda^* \bar{c} c_{|\Omega|} \sup_{\gamma \in \Gamma^*} \|\gamma\|_2 = \lambda^* \bar{c} \Delta c_{|\Omega|}^2 c_p \mathcal{E}(n, p), \quad (24)$$

where the second inequality follows from (17). By setting $t = 8b_1c_p\mathcal{E}(n, p)$ in Lemma 3, we have

$$\text{pr} \left(\Psi^d(S_n) \geq 8b_1c_p\mathcal{E}(n, p) \right) \leq 2p \exp(-2n\mathcal{E}^2(n, p)) \leq 2p \exp(-2\log p) = 2/p \leq \alpha_0.$$

By the definition of λ^* in (8), we have $\lambda^* \leq 8b_1c_0c_p\mathcal{E}(n, p)$, which along with (24) indicates that

$$\lambda^* \sup_{\gamma \in \Gamma^*} \{|\Psi(\gamma + \beta^*) - \Psi(\beta^*)|\} \leq 8b_1c_0\bar{c}\Delta c_{|\Omega|}^2 c_p^2 \mathcal{E}^2(n, p). \quad (25)$$

Finally, by combining (19), (23), (25), and (15), we can see the following inequality

$$\begin{aligned} \inf_{\gamma \in \Gamma^*} \{F_{\lambda^*}(\gamma) - F_{\lambda^*}(0)\} &> \left(b_2b_3\Delta - (20 + 4\sqrt{2})b_1c_0\bar{c} - 8b_1c_0\bar{c} \right) \Delta c_{|\Omega|}^2 c_p^2 \mathcal{E}^2(n, p) \\ &= \left(34b_1c_0\bar{c} - (28 + 4\sqrt{2})b_1c_0\bar{c} \right) \Delta c_{|\Omega|}^2 c_p^2 \mathcal{E}^2(n, p) > 0, \end{aligned}$$

holds with probability at least $1 - \exp(-n\mathcal{E}^2(n, p))$. Based on (14), we conclude that

$$\text{pr} \left(\|\hat{\beta}(\lambda^*) - \beta^*\|_2 \leq \Delta c_{|\Omega|} c_p \mathcal{E}(n, p) \right) \geq 1 - \exp(-n\mathcal{E}^2(n, p)) - \alpha_0.$$

This completes the proof. \square

3 An Efficient Superlinearly Convergent Algorithm

3.1 The Proximal Augmented Lagrangian Method and Its Convergence

In this section, we design an efficient, superlinearly convergent algorithm to solve the general class of convex-regularized rank regression problem, with the group lasso case (3) serving as a representative example. Our approach is a proximal augmented Lagrangian method (PALM) applied to the dual formulation, where the added proximal term ensures that the subproblems are well-posed and enables efficient semismooth Newton updates. With this design, PALM avoids the triple-loop structure required by the state-of-the-art PPMM [Tang et al., 2023], and ensures both efficiency and scalability in high-dimensional problems.

Problem (3) can be equivalently written in the constrained form

$$\min_{s \in \mathbb{R}^n, \beta \in \mathbb{R}^p} \{L(s) + \lambda\Psi(\beta) \mid X\beta - s - y = 0\}. \quad (\text{P}')$$

The dual problem of (3) then becomes

$$\sup_{w \in \mathbb{R}^n} \inf_{s \in \mathbb{R}^n, \beta \in \mathbb{R}^p} \{L(s) + \lambda\Psi(\beta) + \langle w, X\beta - s - y \rangle\} = \sup_{w \in \mathbb{R}^n} \{-\langle y, w \rangle - L^*(w) - \lambda\Psi^*(-\lambda^{-1}X^\top w)\},$$

which leads to the equivalent minimization problem:

$$\min_{w \in \mathbb{R}^n} \{g(w) := \langle y, w \rangle + L^*(w) + \lambda\Psi^*(-\lambda^{-1}X^\top w)\}, \quad (\text{D})$$

where $L^*(\cdot)$ and $\Psi^*(\cdot)$ are the conjugate functions of $L(\cdot)$ and $\Psi(\cdot)$, respectively. In addition, the Karush–Kuhn–Tucker (KKT) conditions associated with (P') and (D) are

$$X\beta - s - y = 0, \quad s = \text{Prox}_L(w + s), \quad \beta = \text{Prox}_{\lambda\Psi}(\beta - X^\top w).$$

To facilitate the development of an augmented Lagrangian type method for solving (D), we adopt the framework in [Rockafellar and Wets \[2009, Examples 11.46 & 11.57\]](#). Specifically, we rewrite problem (D) as the minimization of the function $g(w) = \tilde{g}(w, 0, 0)$, where \tilde{g} is defined as follows

$$\tilde{g}(w, \nu, \phi) := \langle y, w \rangle + L^*(w + \nu) + \lambda \Psi^*(-\lambda^{-1} X^\top w + \lambda^{-1} \phi), \quad \forall (w, \nu, \phi) \in \mathbb{R}^n \times \mathbb{R}^n \times \mathbb{R}^p.$$

The associated Lagrangian function is then given by

$$\begin{aligned} l(w; s, \beta) &= \inf_{\nu \in \mathbb{R}^n, \phi \in \mathbb{R}^p} \left\{ \tilde{g}(w, \nu, \phi) - \langle s, \nu \rangle - \langle \beta, \phi \rangle \right\} \\ &= \inf_{\nu \in \mathbb{R}^n, \phi \in \mathbb{R}^p} \left\{ \langle y, w \rangle + L^*(w + \nu) - \langle s, \nu \rangle + \lambda \Psi^*(-\lambda^{-1} X^\top w + \lambda^{-1} \phi) - \langle \beta, \phi \rangle \right\} \\ &= \langle y, w \rangle - L(s) - \lambda \Psi(\beta) + \langle s, w \rangle - \langle \beta, X^\top w \rangle. \end{aligned} \quad (26)$$

Moreover, given $\sigma > 0$, the augmented Lagrangian function corresponding to (D) is

$$\begin{aligned} \mathcal{L}_\sigma(w; s, \beta) &= \sup_{\nu \in \mathbb{R}^n, \phi \in \mathbb{R}^p} \left\{ l(w; \nu, \phi) - \frac{1}{2\sigma} \|\nu - s\|_2^2 - \frac{1}{2\sigma} \|\phi - \beta\|_2^2 \right\} \\ &= \langle y, w \rangle - e_\sigma L(s + \sigma w) + \frac{1}{2\sigma} \|s + \sigma w\|_2^2 - \frac{1}{2\sigma} \|s\|_2^2 - \lambda e_{\sigma\lambda} \Psi(\beta - \sigma X^\top w) \\ &\quad + \frac{1}{2\sigma} \|\beta - \sigma X^\top w\|_2^2 - \frac{1}{2\sigma} \|\beta\|_2^2, \end{aligned}$$

where $e_\sigma L(\cdot)$ and $e_{\sigma\lambda} \Psi(\cdot)$ denote the Moreau envelopes of $L(\cdot)$ and $\Psi(\cdot)$ with parameter σ and $\sigma\lambda$, respectively, as defined in (4).

A direct application of the classical augmented Lagrangian method (ALM) to problem (D) leads to a subproblem in the w -variable, which requires minimizing the augmented Lagrangian function in the form of:

$$\min_{w \in \mathbb{R}^n} \mathcal{L}_\sigma(w; \tilde{s}, \tilde{\beta}),$$

where the objective is continuously differentiable due to the smoothness of $e_\sigma L(\cdot)$ and $e_{\sigma\lambda} \Psi(\cdot)$. The first-order optimality condition for this problem is given by

$$\begin{aligned} \nabla_w \mathcal{L}_\sigma(w; \tilde{s}, \tilde{\beta}) &= y + \text{Prox}_{\sigma L}(\tilde{s} + \sigma w) - X \text{Prox}_{\sigma\lambda \Psi}(\tilde{\beta} - \sigma X^\top w) \\ &= y + \sigma \text{Prox}_L(\tilde{s}/\sigma + w) - \sigma \lambda X \text{Prox}_\Psi\left(\tilde{\beta}/(\sigma\lambda) - X^\top w/\lambda\right), \end{aligned}$$

Here, the second equality holds because $\text{Prox}_{\sigma f}(\cdot) = \sigma \text{Prox}_f(\cdot/\sigma)$ for any $\sigma > 0$ and any positively 1-homogeneous convex function f . However, solving this equation reliably with Newton-type methods is challenging, as the associated generalized Hessian can be singular or ill-conditioned, leading to numerical instability.

To address this issue while preserving the convergence properties of the ALM framework, we incorporate a proximal term $\frac{\tau}{2\sigma_k} \|w - w^k\|_2^2$ into the subproblem, following the established proximal ALM methodologies in [Rockafellar \[1976b\]](#). This modification improves subproblem conditioning and enhances algorithmic stability. The resulting scheme forms our inexact proximal ALM (PALM) in Algorithm 2.

Algorithm 2 Proximal augmented Lagrangian method for the dual of (3)

Input: Initial point $(w^0, s^0, \beta^0) \in \mathbb{R}^n \times \mathbb{R}^n \times \mathbb{R}^p$; parameters $\sigma_0, \tau > 0$; positive summable sequence $\{\delta_k\}$ with $\delta_k < 1$; stopping tolerance $\text{Tol} > 0$. Let $k = 0$.

repeat

 Compute w^{k+1} by solving:

$$w^{k+1} \approx \arg \min_{w \in \mathbb{R}^n} \left\{ \psi_k(w) := \mathcal{L}_{\sigma_k}(w; s^k, \beta^k) + \frac{\tau}{2\sigma_k} \|w - w^k\|_2^2 \right\} \quad (27)$$

such that

$$\|\nabla \psi_k(w^{k+1})\|_2 \leq \frac{\delta_k \min(1, \sqrt{\tau})}{\sigma_k} \min \left\{ 1, \left\| (\sqrt{\tau}w^{k+1}, s^{k+1}, \beta^{k+1}) - (\sqrt{\tau}w^k, s^k, \beta^k) \right\|_2 \right\}. \quad (28)$$

Compute

$$s^{k+1} = \sigma_k \text{Prox}_L(s^k/\sigma_k + w^{k+1}), \quad \beta^{k+1} = \sigma_k \lambda \text{Prox}_\Psi(\beta^k/(\sigma_k \lambda) - X^\top w^{k+1}/\lambda).$$

Update $\sigma_{k+1} \geq \sigma_k$, and let $k \leftarrow k + 1$.

until the relative KKT residual of (P') and (D) satisfies

$$\eta_{\text{kkt}}(w^{k+1}, s^{k+1}, \beta^{k+1}) := \max\{\eta_p(s^{k+1}, \beta^{k+1}), \eta_d(w^{k+1}, s^{k+1}, \beta^{k+1})\} \leq \text{Tol}, \quad (29)$$

where $\eta_p(s, \beta) := \frac{\|X\beta - s - y\|_2}{1 + \|y\|_2}$ and $\eta_d(w, s, \beta) := \max \left\{ \frac{\|s - \text{Prox}_L(w + s)\|_2}{1 + \|s\|_2}, \frac{\|\beta - \text{Prox}_{\lambda\Psi}(\beta - X^\top w)\|_2}{1 + \|\beta\|_2} \right\}$.

Output: Approximate solution (s^{k+1}, β^{k+1}) to (P'), and approximate solution w^{k+1} to (D).

Remark 3. In practical implementations, we set $\tau = 1$ and update $\sigma_{k+1} = 1.5\sigma_k$. The stopping tolerance is chosen as $\text{Tol} = 10^{-6}$ to ensure high solution accuracy.

Let $\mathcal{M} := \text{Diag}(\tau I_n, I_n, I_p)$ be a block diagonal matrix, where I_n denotes the $n \times n$ identity matrix. We then define the maximal monotone operator \mathcal{T} , induced from the convex-concave Lagrangian function in (26), as

$$\begin{aligned} \mathcal{T}(w, s, \beta) &:= \{(w', s', \beta') \mid (w', -s', -\beta') \in \partial l(w; s, \beta)\} \\ &= \{(w', s', \beta') \mid w' = y + s - X\beta, s' \in -w + \partial L(s), \beta' \in X^\top w + \partial \lambda \Psi(\beta)\}. \end{aligned}$$

Then, each iteration of Algorithm 2 can be equivalently viewed as generating an approximate solution to the inclusion

$$(w^{k+1}, s^{k+1}, \beta^{k+1}) \approx (\mathcal{M} + \sigma_k \mathcal{T})^{-1} \mathcal{M}(w^k, s^k, \beta^k),$$

which places it within the framework of the preconditioned proximal point algorithm and allows us to analyze its convergence using the results in [Li et al., 2020, Theorems 2.3 & 2.5]. Moreover, we can see that $\mathcal{T}^{-1}(0)$, the solution set of the KKT system of (P') and (D), is nonempty and compact [Rockafellar and Wets, 2009, Exercise 12.8]. Since the objective function of Problem (3) is convex piecewise linear-quadratic, the operator \mathcal{T} is a polyhedral multifunction. It therefore satisfies the local error bound condition (see, e.g., Robinson [2009], Li et al. [2020]). In particular, for given $r > \sum_{k=0}^{\infty} \delta_k$, there exists $\kappa > 0$ such that

$$\text{dist}((w, s, \beta), \mathcal{T}^{-1}(0)) \leq \kappa \text{dist}(0, \mathcal{T}(w, s, \beta)), \quad \forall (w, s, \beta) \text{ with } \text{dist}((w, s, \beta), \mathcal{T}^{-1}(0)) \leq r. \quad (30)$$

Based on the above analysis and following the framework from [Li et al. \[2020, Theorems 2.3 & 2.5\]](#), we establish the convergence properties of Algorithm 2 in Theorem 2.

Theorem 2. *Let $\{(w^k, s^k, \beta^k)\}$ be the sequence generated by Algorithm 2. Then $\{(s^k, \beta^k)\}$ converges to an optimal solution of (P') , and $\{w^k\}$ converges to an optimal solution of (D) . Moreover, if the initial point (w^0, s^0, β^0) satisfies*

$$\text{dist}((w^0, s^0, \beta^0), \mathcal{T}^{-1}(0)) \leq r - \sum_{k=0}^{\infty} \delta_k,$$

then it holds that

$$\text{dist}_{\mathcal{M}}\left((w^{k+1}, s^{k+1}, \beta^{k+1}), \mathcal{T}^{-1}(0)\right) \leq \mu_k \text{dist}_{\mathcal{M}}\left((w^k, s^k, \beta^k), \mathcal{T}^{-1}(0)\right),$$

where $\mu_k = (1 - \delta_k)^{-1} \left(\delta_k + (1 + \delta_k) \kappa \gamma / \sqrt{\sigma_k^2 + \kappa^2 \gamma^2} \right)$ with $\gamma := \max\{1, \tau\}$, and constants κ, r are specified in (30).

Note that

$$\mu_{\infty} := \limsup_{k \rightarrow \infty} \mu_k = \frac{\kappa \gamma}{\sqrt{\sigma_{\infty}^2 + \kappa^2 \gamma^2}} < 1,$$

where $\sigma_{\infty} := \lim_{k \rightarrow \infty} \sigma_k$. This implies that Theorem 2 establishes the Q -linear convergence rate of the primal-dual sequence $\{(w^k, s^k, \beta^k)\}$. Moreover, if $\sigma_{\infty} = \infty$, then $\mu_{\infty} = 0$, and the convergence improves to asymptotically Q -superlinear.

3.2 A Semismooth Newton Method for the Subproblem (27)

While PALM in Algorithm 2 enjoys favorable convergence properties, its practical efficiency critically depends on whether the subproblem (27) can be solved efficiently at each iteration. In this subsection, we develop a semismooth Newton (SSN) method to solve (27) with implementation details deferred to the next subsection.

Observing that $\psi_k(w)$ in (27) is strongly convex and differentiable, problem (27) admits a unique optimal solution \bar{w}^{k+1} , which satisfies the associated first-order optimality condition:

$$\nabla \psi_k(w) = y + \sigma_k \text{Prox}_L\left(\frac{s^k}{\sigma_k} + w\right) - \sigma_k \lambda X \text{Prox}_{\Psi}\left(\frac{\beta^k}{\sigma_k \lambda} - \frac{X^T w}{\lambda}\right) + \frac{\tau}{\sigma_k} (w - w^k) = 0. \quad (31)$$

Since both $\text{Prox}_L(\cdot)$ and $\text{Prox}_{\Psi}(\cdot)$ are Lipschitz continuous and piecewise affine (see Section 3.3 for details), the nonlinear equation (31) can be efficiently solved using a SSN method.

To solve (31), we define the following set-valued mapping:

$$\hat{\partial}^2 \psi_k(w) := \sigma_k \partial \text{Prox}_L\left(\frac{s^k}{\sigma_k} + w\right) + \sigma_k X \partial \text{Prox}_{\Psi}\left(\frac{\beta^k}{\sigma_k \lambda} - \frac{X^T w}{\lambda}\right) X^T + \frac{\tau}{\sigma_k} I_n, \quad (32)$$

where $\partial \text{Prox}_L(\cdot)$ and $\partial \text{Prox}_{\Psi}(\cdot)$ denote the Clarke subdifferentials of the proximal operators $\text{Prox}_L(\cdot)$ and $\text{Prox}_{\Psi}(\cdot)$, respectively. It can be seen that $\nabla \psi_k(\cdot)$ is strongly semismooth with respect to $\hat{\partial}^2 \psi_k(w)(\cdot)$, and all elements in $\hat{\partial}^2 \psi_k(w)$ are positive definite for any $w \in \mathbb{R}^n$ (see Section 3.3 for details).

With these preparations in place, we now present the SSN method for solving the nonsmooth equation (31). The algorithm proceeds as follows:

Algorithm 3 Semismooth Newton Method for solving (31)

Input: $\bar{\mu} \in (0, 1/2)$, $\bar{\eta} \in (0, 1)$, $\bar{\tau} \in (0, 1]$, $\bar{\delta} \in (0, 1)$, $w^{(0)} = w^k$, and $j = 0$.

repeat

Choose $\Lambda^{(j)} \in \partial \text{Prox}_L(s^k/\sigma_k + w^{(j)})$ and $V^{(j)} \in \partial \text{Prox}_\Psi(\beta^k/(\sigma_k \lambda) - X^\top w^{(j)}/\lambda)$. Let $H^{(j)} = \sigma_k \Lambda^{(j)} + \sigma_k X V^{(j)} X^\top + \frac{\bar{\tau}}{\sigma_k} I_n$. Solve the following linear system

$$H^{(j)} d = -\nabla \psi_k(w^{(j)}) \quad (33)$$

exactly or approximately by the conjugate gradient (CG) algorithm to find $d^{(j)}$ such that

$$\|H^{(j)} d^{(j)} + \nabla \psi_k(w^{(j)})\|_2 \leq \min\{\bar{\eta}, \|\nabla \psi_k(w^{(j)})\|_2^{1+\bar{\tau}}\}.$$

Set $\alpha_{(j)} = \bar{\delta}^{m_{(j)}}$, where $m_{(j)}$ is the first nonnegative integer m for which

$$\psi_k(w^{(j)} + \bar{\delta}^m d^{(j)}) \leq \psi_k(w^{(j)}) + \bar{\mu} \bar{\delta}^m \langle \nabla \psi_k(w^{(j)}), d^{(j)} \rangle.$$

Step 3: Set $w^{(j+1)} = w^{(j)} + \alpha_{(j)} d^{(j)}$, $j \leftarrow j + 1$.

until condition (28) is satisfied.

Output: Solution $w^{(j)}$ as w^{k+1} in (27).

Remark 4. In practical implementations, we set $\bar{\mu} = 10^{-3}$, $\bar{\eta} = 10^{-1}$, $\bar{\tau} = 10^{-1}$, and $\bar{\delta} = 0.5$.

The convergence result of the SSN method in Algorithm 3 is provided in the following theorem, which is a direct consequence of Zhao et al. [2010, Proposition 3.3 & Theorem 3.4] and Li et al. [2018, Theorem 3].

Theorem 3. Let $\{w^{(j)}\}$ be the sequence generated by Algorithm 3. Then $\{w^{(j)}\}$ converges to the unique optimal solution \bar{w}^{k+1} of problem (27) and

$$\|w^{(j+1)} - \bar{w}^{k+1}\|_2 = \mathcal{O}(\|w^{(j)} - \bar{w}^{k+1}\|_2^{1+\bar{\tau}}),$$

where $\bar{\tau} \in (0, 1]$ is given in the algorithm.

3.3 Implementation Details of the Semismooth Newton Method

The main computational cost of the proposed semismooth Newton method in Algorithm 3 comes from solving the $n \times n$ Newton system (33), which highly depends on the structure of the chosen generalized Hessian matrix $H^{(j)}$ from (32). To enable an efficient implementation, we first characterize the proximal mappings associated with the loss function $L(\cdot)$ and the regularizer $\Psi(\cdot)$, together with their generalized Jacobians.

We recall that $L(\cdot)$, also known as the *clustered lasso regularizer*, has been studied in Lin et al. [2019], where the proximal mapping and its generalized Jacobian were characterized. Building on these results, we present the following proposition. For convenience, we define the polyhedral cone $\mathcal{D} := \{s \in \mathbb{R}^n \mid \Delta s \geq 0\}$, where $\Delta \in \mathbb{R}^{(n-1) \times n}$ is the difference operator given by $\Delta s = (s_1 - s_2, \dots, s_{n-1} - s_n)^\top$ for any $s \in \mathbb{R}^n$.

Proposition 1. *Given any $s \in \mathbb{R}^n$, let s^\downarrow denote its nonincreasing rearrangement, with the permutation matrix P_s such that $s^\downarrow = P_s s$. Then the following results hold.*

(i) *The proximal mapping of $L(\cdot)$ can be computed by*

$$\text{Prox}_L(s) = P_s^\top \Pi_{\mathcal{D}}(P_s s - \varrho),$$

where $\varrho_k = \frac{2n - 4k + 2}{n(n-1)}$ for $k \in [n]$, and $\Pi_{\mathcal{D}}$ is the projection onto the cone \mathcal{D} , computable via the pool-adjacent-violators algorithm [Best and Chakravarti, 1990].

(ii) *For $z \in \mathbb{R}^n$, we define the active set $\mathcal{I}_{\mathcal{D}}(z) := \{i \in [n-1] \mid (\Delta \Pi_{\mathcal{D}}(z))_i = 0\}$, the multiplier set $\mathcal{M}_{\mathcal{D}}(z) = \{\lambda \in \mathbb{R}_-^{n-1} \mid \Delta^\top \lambda = z - \Pi_{\mathcal{D}}(z), \lambda_i = 0 \text{ for } i \notin \mathcal{I}_{\mathcal{D}}(z)\}$, and the index set*

$$\mathcal{K}_{\mathcal{D}}(z) := \{K \subseteq [n-1] \mid \exists \lambda \in \mathcal{M}_{\mathcal{D}}(z) \text{ s.t. } \text{supp}(\lambda) \subseteq K \subseteq \mathcal{I}_{\mathcal{D}}(z)\}.$$

Then we have the following generalized Jacobian of $\text{Prox}_L(s)$:

$$\partial \text{Prox}_L(s) = \{\Lambda \in \mathbb{R}^{n \times n} \mid \Lambda = I_n - P_s^\top \Delta_K^\top (\Delta_K \Delta_K^\top)^{-1} \Delta_K P_s, K \in \mathcal{K}_{\mathcal{D}}(P_s s - \varrho)\},$$

where Δ_K is the matrix consisting of the rows of Δ indexed by K .

(iii) *$\text{Prox}_L(\cdot)$ is strongly semismooth with respect to $\partial \text{Prox}_L(\cdot)$.*

(iv) *Define $\theta \in \mathbb{R}^{n-1}$ as $\theta_i = 1$ if $i \in \mathcal{I}_{\mathcal{D}}(P_s s - \varrho)$, and 0 otherwise. Consider the block decomposition of θ into N consecutive blocks: $\theta = (\theta^{(1)}; \dots; \theta^{(N)})$, where each $\theta^{(i)} = 0_{n_i}$ or 1_{n_i} , with $\sum_{i=1}^N n_i = n-1$ and adjacent blocks taking different values. Define the active block index set $\mathcal{J}^s = \{i \in [N] \mid \theta^{(i)} = 1_{n_i}\}$, listed in increasing order with its j th element denoted as \mathcal{J}_j^s . Then we can construct:*

$$\Lambda(s) = \text{Diag}(P_s^\top \theta_s) + P_s^\top \Gamma_s \Gamma_s^\top P_s \in \partial \text{Prox}_L(s),$$

where $\theta_s = (\theta_s^{(1)}; \dots; \theta_s^{(N)}) \in \mathbb{R}^n$ is defined as:

$$\theta_s^{(i)} = \begin{cases} 0_{n_i+1} & \text{if } i \in \mathcal{J}^s, \\ 1_{n_i} & \text{if } i \in \{1, N\} \setminus \mathcal{J}^s, \\ 1_{n_i-1} & \text{otherwise,} \end{cases}$$

and the matrix $\Gamma_s \in \mathbb{R}^{n \times |\mathcal{J}^s|}$ is defined by:

$$(\Gamma_s)_{\ell,j} = \begin{cases} \frac{1}{\sqrt{n_{\mathcal{J}_j^s} + 1}} & \text{if } \sum_{t=1}^{\mathcal{J}_j^s-1} n_t + 1 \leq \ell \leq \sum_{t=1}^{\mathcal{J}_j^s} n_t, \\ 0 & \text{otherwise,} \end{cases} \quad \ell \in [n], j \in [|\mathcal{J}^s|].$$

For the group lasso regularizer $\Psi(\cdot)$, both the proximal operator and its generalized Jacobian admits a separable structure across groups. This result is stated in the following proposition, adapted from Zhang et al. [2020].

Proposition 2. For any $\beta \in \mathbb{R}^p$, the following results hold.

(i) The proximal operator of the group lasso regularizer $\Psi(\cdot)$ satisfies:

$$(\text{Prox}_\Psi(\beta))_{\mathcal{G}_l} = \text{Prox}_{w_l \|\cdot\|_2}(\beta_{\mathcal{G}_l}) = \beta_{\mathcal{G}_l} - \Pi_{\mathcal{B}_2^{w_l}}(\beta_{\mathcal{G}_l}), \quad l \in [g],$$

where $\Pi_{\mathcal{B}_2^{w_l}}$ is the projection onto $\mathcal{B}_2^{w_l}$, computable as $\Pi_{\mathcal{B}_2^{w_l}}(\varpi) = \varpi / \max\{1, \|\varpi\|_2/w_l\}$.

(ii) For $l \in [g]$, define the linear operator $\mathcal{P}_l : \mathbb{R}^p \rightarrow \mathbb{R}^{|\mathcal{G}_l|}$ by $\mathcal{P}_l x = x_{\mathcal{G}_l}$ and set $\mathcal{P} := (\mathcal{P}_1; \dots; \mathcal{P}_g)$. Then the Clarke generalized Jacobian of $\text{Prox}_\Psi(\beta)$ is:

$$\partial \text{Prox}_\Psi(\beta) = \left\{ I_p - \mathcal{P}^\top \Sigma \mathcal{P} \mid \Sigma = \text{Diag}(\Sigma_1, \dots, \Sigma_g), \Sigma_l \in \partial \Pi_{\mathcal{B}_2^{w_l}}(\beta_{\mathcal{G}_l}), l \in [g] \right\},$$

where

$$\partial \Pi_{\mathcal{B}_2^{w_l}}(\varpi) = \begin{cases} \frac{w_l}{\|\varpi\|_2} \left(I_{|\mathcal{G}_l|} - \frac{\varpi \varpi^\top}{\|\varpi\|_2^2} \right), & \text{if } \|\varpi\|_2 > w_l, \\ \left\{ I_{|\mathcal{G}_l|} - t \frac{\varpi \varpi^\top}{(w_l)^2} \mid 0 \leq t \leq 1 \right\}, & \text{if } \|\varpi\|_2 = w_l, \\ I_{|\mathcal{G}_l|}, & \text{otherwise.} \end{cases}$$

(iii) $\text{Prox}_\Psi(\cdot)$ is strongly semismooth with respect to $\partial \text{Prox}_\Psi(\cdot)$.

(iv) We construct $V(\beta) = \sum_{l \in \mathcal{R}^\beta} V_l \in \partial \text{Prox}_\Psi(\beta)$, where $\mathcal{R}^\beta := \{l \in [g] \mid \|\beta_{\mathcal{G}_l}\|_2 > w_l\}$, and

$$V_l = \left(1 - \frac{w_l}{\|\beta_{\mathcal{G}_l}\|_2} \right) \text{Diag}(\eta^l) + \frac{w_l}{\|\beta_{\mathcal{G}_l}\|_2^3} (\mathcal{P}_l^\top \beta_{\mathcal{G}_l}) (\mathcal{P}_l^\top \beta_{\mathcal{G}_l})^\top, \quad l \in \mathcal{R}^\beta,$$

with $\eta^l \in \mathbb{R}^p$ defining as $(\eta^l)_i = 1$ if $i \in \mathcal{G}_l$ and 0 otherwise.

With the established results in Propositions 1 and 2, we now present the computational details for solving the Newton equation (33). For brevity, we write $\tilde{s} = s^k/\sigma_k + w^{(j)}$, $\tilde{\beta} = \beta^k/(\sigma_k \lambda) - X^\top w^{(j)}/\lambda$. By taking

$$\Lambda^{(j)} = \Lambda(\tilde{s}) \in \partial \text{Prox}_L(\tilde{s}), \quad V^{(j)} = V(\tilde{\beta}) \in \text{Prox}_\Psi(\tilde{\beta}),$$

the linear operator $H^{(j)}$ in (33) becomes

$$\begin{aligned} H^{(j)} &= \frac{\tau}{\sigma_k} I_n + \sigma_k \Lambda(\tilde{s}) + \sigma_k X V^{(j)} X^\top \\ &= \frac{\tau}{\sigma_k} I_n + \sigma_k \left(\text{Diag}(P_{\tilde{s}}^\top \theta_{\tilde{s}}) + P_{\tilde{s}}^\top \Gamma_{\tilde{s}} \Gamma_{\tilde{s}}^\top P_{\tilde{s}} \right) \\ &\quad + \sigma_k \sum_{l \in \mathcal{R}^{\tilde{s}}} X \left(\left(1 - \frac{w_l}{\|\tilde{\beta}_{\mathcal{G}_l}\|_2} \right) \text{Diag}(\eta^l) + \frac{w_l}{\|\tilde{\beta}_{\mathcal{G}_l}\|_2^3} (\mathcal{P}_l^\top \tilde{\beta}_{\mathcal{G}_l}) (\mathcal{P}_l^\top \tilde{\beta}_{\mathcal{G}_l})^\top \right) X^\top. \end{aligned}$$

Noting the nature of the linear operators \mathcal{P}_l , $l \in [g]$ and the 0-1 structure of the vectors η^l , $l \in \mathcal{R}^{\tilde{s}}$, we can see that

$$H^{(j)} = \frac{\tau}{\sigma_k} I_n + \sigma_k \text{Diag}(P_{\tilde{s}}^\top \theta_{\tilde{s}}) + \sigma_k [\Theta, \Xi, \Upsilon] \begin{bmatrix} \Theta^\top \\ \Xi^\top \\ \Upsilon^\top \end{bmatrix}, \quad (34)$$

where $\Theta = P_{\tilde{s}}^T \Gamma_{\tilde{s}} \in \mathbb{R}^{n \times |\mathcal{J}^{\tilde{s}}|}$, and

$$\Xi = [\Xi_1, \dots, \Xi_{|\mathcal{R}^{\tilde{\beta}}|}] \in \mathbb{R}^{n \times \sum_{l \in \mathcal{R}^{\tilde{\beta}}} |\mathcal{G}_l|} \quad \text{with} \quad \Xi_l = \sqrt{1 - \frac{w_l}{\|\tilde{\beta}_{\mathcal{G}_l}\|_2}} X_l \in \mathbb{R}^{n \times |\mathcal{G}_l|}, \quad l \in \mathcal{R}^{\tilde{\beta}},$$

$$\Upsilon = [\Upsilon_1, \dots, \Upsilon_{|\mathcal{R}^{\tilde{\beta}}|}] \in \mathbb{R}^{n \times |\mathcal{R}^{\tilde{\beta}}|} \quad \text{with} \quad \Upsilon_l = \sqrt{\frac{w_l}{\|\tilde{\beta}_{\mathcal{G}_l}\|_2^3}} (X_l \tilde{\beta}_{\mathcal{G}_l}) \in \mathbb{R}^n, \quad l \in \mathcal{R}^{\tilde{\beta}},$$

with $X_l \in \mathbb{R}^{n \times |\mathcal{G}_l|}$ being the submatrix of X with those columns in \mathcal{G}_l .

Then the computational complexity of solving the linear system (33) with coefficient matrix $H^{(j)}$ in (34) can be separated into two stages. In the first stage, the required components in $H^{(j)}$ are prepared: forming the vector $P_{\tilde{s}}^T \theta_{\tilde{s}}$ and the matrix Θ requires no arithmetic cost as they can be obtained by reordering, and computing the matrices Ξ and Υ requires $\mathcal{O}(n \sum_{l \in \mathcal{R}^{\tilde{\beta}}} |\mathcal{G}_l|)$ operations. In the second stage, the system (33) can be solved by several alternative strategies, depending on the relative values of n and

$$r := |\mathcal{J}^{\tilde{s}}| + \sum_{l \in \mathcal{R}^{\tilde{\beta}}} |\mathcal{G}_l| + |\mathcal{R}^{\tilde{\beta}}|,$$

which characterizes the problem sparsity: $|\mathcal{J}^{\tilde{s}}|$ reflects the sparsity induced by the rank loss, $\sum_{l \in \mathcal{R}^{\tilde{\beta}}} |\mathcal{G}_l|$ corresponds to the solution sparsity, and $|\mathcal{R}^{\tilde{\beta}}|$ captures the group sparsity. The most direct approach is to explicitly form $H^{(j)}$, which costs $\mathcal{O}(n^2 r)$, followed by a direct solver with complexity $\mathcal{O}(n^3)$. When n is large, a more suitable option is the CG method, where each matrix-vector multiplication $H^{(j)} d$ requires $\mathcal{O}(nr)$ operations. If $r \ll n$, the low-rank structure of $H^{(j)}$ can be further exploited to solve the linear system through the Sherman-Morrison-Woodbury formula, leading to an overall complexity of $\mathcal{O}(nr^2 + r^3)$. Overall, the sparsity structure encoded in r plays a key role in reducing computational cost and enables the Newton system to be solved efficiently.

4 Numerical Experiments

4.1 Overview of Experimental Design

This section presents comprehensive numerical studies to evaluate the proposed group lasso regularized rank regression model in terms of statistical performance, and to assess the proposed algorithm in terms of computational efficiency. We begin by examining the estimation accuracy and robustness of the group lasso regularized rank regression model with the data-driven parameter selection under various data-generating processes, comparing its performance against several commonly used models. On the computational side, we conduct two complementary studies. The first evaluates the scalability of the proposed proximal augmented Lagrangian method (PALM) with an SSN inner solver for solving the group lasso regularized rank regression. The second benchmarks PALM on ℓ_1 -regularized rank regression against a state-of-the-art method, highlighting the broader applicability of our framework to general nonsmooth convex regularizers. All experiments were performed in MATLAB on an Apple M3 system running macOS (version 15.3.1) with 24 GB of RAM.

4.2 Statistical Performance of Group Lasso Regularized Rank Regression

We compare the performance of our proposed group lasso regularized rank regression model (3) (Rank_GLasso) against two alternatives: the group lasso regularized least squares regression model

[Yuan and Lin, 2006] (LS_GLasso) and the ℓ_1 regularized rank regression model [Wang et al., 2020] (Rank_Lasso). Each model involves a single regularization parameter λ , but the choice of λ differs across methods. For Rank_GLasso, λ is computed by Algorithm 1 without additional tuning. For Rank_Lasso, we adopt the quantile-based selection rule¹ proposed in Wang et al. [2020]. It is worth noting that our Algorithm 1 generalizes this rule to the group lasso setting: when the regularizer Ψ in (8) is chosen as the ℓ_1 -norm, their method is recovered as a special case. For LS_GLasso, the regularization parameter λ is selected via 5-fold cross-validation over 10 logarithmically spaced values between $\lambda_{\max} = \max_{1 \leq l \leq g} \|X_{G_l}^\top y\|_2 / \sqrt{|G_l|}$ and $10^{-4}\lambda_{\max}$. The value that minimizes the validation mean squared error is chosen.

We use the proposed Algorithm 2 to solve Rank_GLasso and Rank_Lasso, each with its corresponding Ψ function. For LS_GLasso, we adopt the state-of-the-art solver² from Zhang et al. [2020] for sparse group lasso regularized least squares regression problems. All methods are terminated when the relative KKT residual $\eta_{\text{kkt}} \leq 10^{-6}$, where η_{kkt} is defined by (29) for Rank_GLasso and Rank_Lasso, and follows the definition in Zhang et al. [2020] for LS_GLasso.

Data Generation. To systematically evaluate the competing models, we adopt the linear regression framework (1) and generate synthetic data by specifying the distributions of covariates, true coefficient vector, and noise. The rows of the design matrix X are sampled i.i.d. from the p -dimensional multivariate Gaussian distribution $\mathcal{N}(0, \Sigma)$, where the covariance structure Σ is chosen from two settings:

- (C1) Equi-correlation: $\Sigma_{ij} = 0.3$ for all $i \neq j$, and $\Sigma_{ii} = 1$ for $i = j$.
- (C2) Auto-regressive (AR(1)): $\Sigma_{ij} = 0.9^{|i-j|}$.

The true coefficient vector $\beta^* \in \mathbb{R}^p$ exhibits group sparsity. We partition the covariates into $g = p/20$ non-overlapping groups $\mathcal{G} = \{G_1, \dots, G_g\}$, among which only 1% of groups are active, i.e., contain nonzero coefficients. For simplicity, the active groups are taken to be the first m groups in \mathcal{G} . We consider two signal patterns:

- (S1) Uniform signal: $(\beta^*)_{G_l} = \sqrt{3}e_{|G_l|}$, $l \in [m]$.
- (S2) Linear decaying signal: $(\beta^*)_{G_l} = (2 - (j-1)/4)e_{|G_l|}$, $j \in [|G_l|]$, $l \in [m]$.

We consider six different noise distributions, including three Gaussian variants and three heavy-tailed alternatives. For all $i \in [n]$, each noise ϵ_i is drawn i.i.d. from the specified distribution.

- (E1) Gaussian noise with low variance: $\mathcal{N}(0, 0.25)$;
- (E2) Gaussian noise with standard variance: $\mathcal{N}(0, 1)$;
- (E3) Gaussian noise with high variance: $\mathcal{N}(0, 2)$;
- (E4) Gaussian mixture with outliers: $\mathcal{N}_{\text{mix}} := 0.95\mathcal{N}(0, 1) + 0.05\mathcal{N}(0, 100)$;
- (E5) Student's t-distribution with 4 degrees of freedom: $\sqrt{2}t_4$;
- (E6) Cauchy distribution: $\text{Cauchy}(0, 1)$.

Estimation accuracy metric. We evaluate the estimation performance of the competing models using the following three metrics. The first is the ℓ_2 error, defined as $\|\hat{\beta} - \beta^*\|_2$, which measures the Euclidean distance between the estimated coefficient vector $\hat{\beta}$ and the true coefficient vector β^* . The second is the model error (ME), given by $(\hat{\beta} - \beta^*)^\top \Sigma_X (\hat{\beta} - \beta^*)$, where Σ_X is the

¹TFRE package: <https://github.com/yunanwu123/TFRE>

²<https://github.com/YangjingZhang/SparseGroupLasso>

sample covariance matrix of the design matrix X . This metric quantifies the prediction discrepancy with respect to the observed design. The third metric assesses the support recovery performance through the number of false positives (FP) and false negatives (FN). Specifically, FP is the count of incorrectly selected variables, computed as $\sum_{j=1}^p \mathbf{1}(\beta_j^* = 0 \text{ and } \hat{\beta}_j \neq 0)$, while FN is the count of missed true variables, computed as $\sum_{j=1}^p \mathbf{1}(\beta_j^* \neq 0 \text{ and } \hat{\beta}_j = 0)$.

Table 1: Comparison of models in terms of estimation accuracy on data generated with X under covariance structure (C1) and β^* under signal pattern (S1) across all noise distributions (E1)–(E6)

| Noise | Method | λ | Time | ℓ_2 Error | ME | FP | FN |
|----------------------------|-------------|-----------|-------|----------------|---------|------|----|
| $\mathcal{N}(0, 0.25)$ | LS_GLasso | 4.784 | 01:00 | 5.22e-1 | 1.28e-1 | 1056 | 0 |
| | Rank_Lasso | 0.191 | 00:02 | 1.53e+1 | 1.72e+2 | 0 | 75 |
| | Rank_GLasso | 0.071 | 00:02 | 6.75e-1 | 2.38e-1 | 0 | 0 |
| $\mathcal{N}(0, 1)$ | LS_GLasso | 11.655 | 01:07 | 9.68e-1 | 3.99e-1 | 814 | 0 |
| | Rank_Lasso | 0.190 | 00:01 | 1.54e+1 | 1.55e+2 | 0 | 78 |
| | Rank_GLasso | 0.070 | 00:02 | 1.47e+0 | 1.06e+0 | 0 | 0 |
| $\mathcal{N}(0, 2)$ | LS_GLasso | 10.635 | 01:20 | 1.40e+0 | 1.16e+0 | 1168 | 0 |
| | Rank_Lasso | 0.189 | 00:01 | 1.54e+1 | 1.49e+2 | 0 | 78 |
| | Rank_GLasso | 0.071 | 00:02 | 1.91e+0 | 1.90e+0 | 0 | 0 |
| \mathcal{N}_{mix} | LS_GLasso | 27.798 | 01:26 | 3.59e+0 | 5.55e+0 | 1006 | 0 |
| | Rank_Lasso | 0.190 | 00:01 | 1.55e+1 | 1.44e+2 | 0 | 78 |
| | Rank_GLasso | 0.071 | 00:03 | 2.47e+0 | 2.93e+0 | 0 | 0 |
| $\sqrt{2}t_4$ | LS_GLasso | 12.791 | 01:18 | 1.38e+0 | 1.22e+0 | 985 | 0 |
| | Rank_Lasso | 0.191 | 00:01 | 1.55e+1 | 1.82e+2 | 0 | 80 |
| | Rank_GLasso | 0.070 | 00:02 | 1.42e+0 | 1.20e+0 | 0 | 0 |
| Cauchy(0, 1) | LS_GLasso | 396.878 | 01:39 | 1.44e+1 | 1.75e+2 | 658 | 10 |
| | Rank_Lasso | 0.190 | 00:01 | 1.55e+1 | 1.81e+2 | 0 | 80 |
| | Rank_GLasso | 0.071 | 00:03 | 3.35e+0 | 6.92e+0 | 0 | 0 |

Table 2: Comparison of models in terms of estimation accuracy on data generated with X under covariance structure (C1) and β^* under signal pattern (S2) across all error distributions (E1)–(E6)

| Noise | Method | λ | Time | ℓ_2 Error | ME | FP | FN |
|----------------------------|-------------|-----------|-------|----------------|---------|------|----|
| $\mathcal{N}(0, 0.25)$ | LS_GLasso | 12.506 | 01:08 | 5.13e-1 | 1.28e-1 | 146 | 0 |
| | Rank_Lasso | 0.191 | 00:01 | 1.46e+1 | 1.53e+2 | 0 | 74 |
| | Rank_GLasso | 0.071 | 00:02 | 6.72e-1 | 2.36e-1 | 0 | 0 |
| $\mathcal{N}(0, 1)$ | LS_GLasso | 13.395 | 01:16 | 9.57e-1 | 3.75e-1 | 753 | 0 |
| | Rank_Lasso | 0.190 | 00:01 | 1.46e+1 | 1.43e+2 | 0 | 75 |
| | Rank_GLasso | 0.070 | 00:02 | 1.46e+0 | 1.05e+0 | 0 | 0 |
| $\mathcal{N}(0, 2)$ | LS_GLasso | 12.076 | 01:20 | 1.39e+0 | 1.08e+0 | 1095 | 0 |
| | Rank_Lasso | 0.189 | 00:01 | 1.46e+1 | 1.33e+2 | 0 | 77 |
| | Rank_GLasso | 0.071 | 00:02 | 1.90e+0 | 1.88e+0 | 0 | 0 |
| \mathcal{N}_{mix} | LS_GLasso | 30.769 | 01:23 | 3.53e+0 | 5.27e+0 | 976 | 0 |
| | Rank_Lasso | 0.190 | 00:01 | 1.47e+1 | 1.31e+2 | 0 | 79 |
| | Rank_GLasso | 0.071 | 00:03 | 2.44e+0 | 2.86e+0 | 0 | 0 |
| $\sqrt{2}t_4$ | LS_GLasso | 14.546 | 01:14 | 1.36e+0 | 1.12e+0 | 951 | 0 |
| | Rank_Lasso | 0.191 | 00:01 | 1.47e+1 | 1.65e+2 | 0 | 78 |
| | Rank_GLasso | 0.070 | 00:02 | 1.41e+0 | 1.18e+0 | 0 | 0 |
| Cauchy(0, 1) | LS_GLasso | 399.078 | 01:33 | 1.39e+1 | 1.65e+2 | 654 | 31 |
| | Rank_Lasso | 0.190 | 00:01 | 1.47e+1 | 1.64e+2 | 0 | 77 |
| | Rank_GLasso | 0.071 | 00:04 | 3.32e+0 | 6.81e+0 | 0 | 0 |

To provide a comprehensive comparison, we consider all combinations of the covariance structures (C1–C2) for X , the signal patterns (S1–S2) for β^* , and the noise distributions (E1–E6) with $n = 500$ and $p = 8000$. The corresponding results are summarized in Tables 1–4, each table focusing on a specific (covariance, signal) setting. This design ensures that both covariance patterns in the covariates and sparsity structures in the true coefficients are systematically examined under a variety of noise distributions. For each setting, we compare the three models by presenting their estimation accuracy metrics, computation time, and the selected regularization parameter λ . The reported computation time includes both the cost of determining λ and the time spent running the algorithm.

As one can see from Tables 1–4, LS_GLasso, which selects the regularization parameter via cross-validation, requires substantially more computational time than Rank_Lasso and Rank_GLasso. This is expected, since cross-validation involves solving multiple optimization problems, whereas the latter models determine the parameter directly from the data without cross-validation, requiring only a single solve. In terms of estimation accuracy, the proposed Rank_GLasso performs comparably to the benchmark LS_GLasso in all cases. Notably, under the heavy-tailed noise setting (E6) with Cauchy(0, 1), Rank_GLasso achieves the best performance among all models, demonstrating strong robustness to extreme outliers. It is worth emphasizing that LS_GLasso is the most widely used approach for regression problems with group sparsity, but it requires cross-validation to select the regularization parameter, which is computationally demanding. By contrast, Rank_GLasso avoids cross-validation by directly computing the parameter within the algorithm, thereby saving substantial time while achieving similarly strong accuracy. The performance of Rank_Lasso is less competitive in terms of ℓ_2 error and ME, which is consistent with its design for element-

wise sparsity rather than group structure. In addition, Rank_GLasso outperforms both LS_GLasso and Rank_Lasso in support recovery. Across all settings, LS_GLasso exhibits a higher FP error, while under (C1), Rank_Lasso suffers from a higher FN error. Overall, the results indicate that Rank_GLasso is both efficient and accurate. It avoids the costly parameter tuning required by LS_GLasso while achieving comparable or superior estimation accuracy across a wide range of experimental settings.

Table 3: Comparison of models in terms of estimation accuracy on data generated with X under covariance structure (C2) and β^* under signal pattern (S1) across all error distributions (E1)–(E6)

| Noise | Method | λ | Time | ℓ_2 Error | ME | FP | FN |
|----------------------------|-------------|-----------|-------|----------------|---------|-----|----|
| $\mathcal{N}(0, 0.25)$ | LS_GLasso | 13.302 | 00:38 | 5.03e-1 | 4.33e-2 | 468 | 0 |
| | Rank_Lasso | 0.222 | 00:02 | 8.31e-1 | 1.10e-1 | 0 | 0 |
| | Rank_GLasso | 0.149 | 00:03 | 4.76e-1 | 5.15e-2 | 0 | 0 |
| $\mathcal{N}(0, 1)$ | LS_GLasso | 37.076 | 00:45 | 6.89e-1 | 1.21e-1 | 119 | 0 |
| | Rank_Lasso | 0.222 | 00:01 | 1.60e+0 | 4.51e-1 | 1 | 0 |
| | Rank_GLasso | 0.150 | 00:02 | 5.98e-1 | 1.78e-1 | 0 | 0 |
| $\mathcal{N}(0, 2)$ | LS_GLasso | 33.374 | 00:53 | 1.22e+0 | 3.07e-1 | 686 | 0 |
| | Rank_Lasso | 0.222 | 00:01 | 2.20e+0 | 7.77e-1 | 1 | 0 |
| | Rank_GLasso | 0.151 | 00:02 | 8.45e-1 | 2.33e-1 | 0 | 0 |
| \mathcal{N}_{mix} | LS_GLasso | 84.269 | 00:59 | 1.71e+0 | 1.22e+0 | 486 | 0 |
| | Rank_Lasso | 0.220 | 00:02 | 2.23e+0 | 9.65e-1 | 0 | 0 |
| | Rank_GLasso | 0.150 | 00:02 | 9.54e-1 | 3.42e-1 | 0 | 0 |
| $\sqrt{2}t_4$ | LS_GLasso | 39.463 | 00:58 | 1.17e+0 | 3.10e-1 | 528 | 0 |
| | Rank_Lasso | 0.225 | 00:02 | 1.97e+0 | 5.35e-1 | 0 | 0 |
| | Rank_GLasso | 0.153 | 00:02 | 7.44e-1 | 1.65e-1 | 0 | 0 |
| Cauchy(0, 1) | LS_GLasso | 879.055 | 01:13 | 4.00e+0 | 3.56e+1 | 203 | 0 |
| | Rank_Lasso | 0.222 | 00:02 | 4.57e+0 | 3.04e+0 | 0 | 0 |
| | Rank_GLasso | 0.153 | 00:02 | 9.61e-1 | 5.66e-1 | 0 | 0 |

Table 4: Comparison of models in terms of estimation accuracy on data generated with X under covariance structure (C2) and β^* under signal pattern (S2) across all error distributions (E1)–(E6)

| Noise | Method | λ | Time | ℓ_2 Error | ME | FP | FN |
|----------------------------|-------------|-----------|-------|----------------|---------|-----|----|
| $\mathcal{N}(0, 0.25)$ | LS_GLasso | 12.519 | 00:43 | 5.00e-1 | 4.52e-2 | 579 | 0 |
| | Rank_Lasso | 0.222 | 00:02 | 8.30e-1 | 1.10e-1 | 0 | 0 |
| | Rank_GLasso | 0.149 | 00:02 | 4.69e-1 | 5.08e-2 | 0 | 0 |
| $\mathcal{N}(0, 1)$ | LS_GLasso | 37.510 | 00:49 | 6.79e-1 | 1.20e-1 | 118 | 0 |
| | Rank_Lasso | 0.222 | 00:02 | 1.60e+0 | 4.51e-1 | 1 | 0 |
| | Rank_GLasso | 0.150 | 00:02 | 5.87e-1 | 1.76e-1 | 0 | 0 |
| $\mathcal{N}(0, 2)$ | LS_GLasso | 33.829 | 00:54 | 1.17e+0 | 2.94e-1 | 684 | 0 |
| | Rank_Lasso | 0.222 | 00:01 | 2.20e+0 | 7.77e-1 | 1 | 0 |
| | Rank_GLasso | 0.151 | 00:02 | 8.10e-1 | 2.28e-1 | 0 | 0 |
| \mathcal{N}_{mix} | LS_GLasso | 85.565 | 01:02 | 1.65e+0 | 1.20e+0 | 464 | 0 |
| | Rank_Lasso | 0.220 | 00:02 | 2.23e+0 | 9.65e-1 | 0 | 0 |
| | Rank_GLasso | 0.150 | 00:02 | 9.19e-1 | 3.35e-1 | 0 | 0 |
| $\sqrt{2}t_4$ | LS_GLasso | 40.067 | 00:51 | 1.13e+0 | 2.98e-1 | 529 | 0 |
| | Rank_Lasso | 0.225 | 00:02 | 1.97e+0 | 5.35e-1 | 0 | 0 |
| | Rank_GLasso | 0.153 | 00:02 | 7.12e-1 | 1.59e-1 | 0 | 0 |
| Cauchy(0, 1) | LS_GLasso | 887.449 | 01:12 | 3.80e+0 | 3.40e+1 | 168 | 0 |
| | Rank_Lasso | 0.222 | 00:02 | 4.57e+0 | 3.04e+0 | 0 | 0 |
| | Rank_GLasso | 0.153 | 00:02 | 9.22e-1 | 5.57e-1 | 0 | 0 |

4.3 Scalability of PALM for Group Lasso Regularized Rank Regression

In this subsection, we examine the scalability of our proposed PALM algorithm for solving the group lasso regularized rank regression model (3). Data are generated as described in Section 4.2, where X follows structure (C1), and β^* follows signal pattern (S1), modified by setting $g = p/100$ instead of $p/20$ to accommodate higher-dimensional settings while maintaining a reasonable number of groups. Experiments are conducted under noise distributions (E1)–(E6).

To systematically assess scalability, we conduct two sets of experiments. In the first, the sample size n is fixed while the dimension p increases from moderately large ($p = 50000$) to extremely high ($p = 400000$). To illustrate the role of sample size, we consider both $n = 500$ and $n = 2000$. The results, summarized in Fig. 1, show that computation time grows nearly linearly with the dimension p across all noise settings. Even at the largest scale ($p = 400000$), PALM remains robust and efficient, underscoring its practical applicability in very high-dimensional problems.

In the second set of experiments, we fix the dimension p and increase the sample size n to examine the effect of sample growth. Two representative dimensions are considered, $p = 8000$ and $p = 100000$, with n varying from 250 to 2000. The results are summarized in Fig. 2. The computation time increases steadily with n , yet the relative growth remains moderate. This demonstrates that PALM scales well with sample size and can efficiently handle large datasets while maintaining reasonable computational costs.

Collectively, these results demonstrate the robust scalability of PALM across both dimensionality and sample size. Under diverse noise distributions, PALM exhibits nearly linear computational

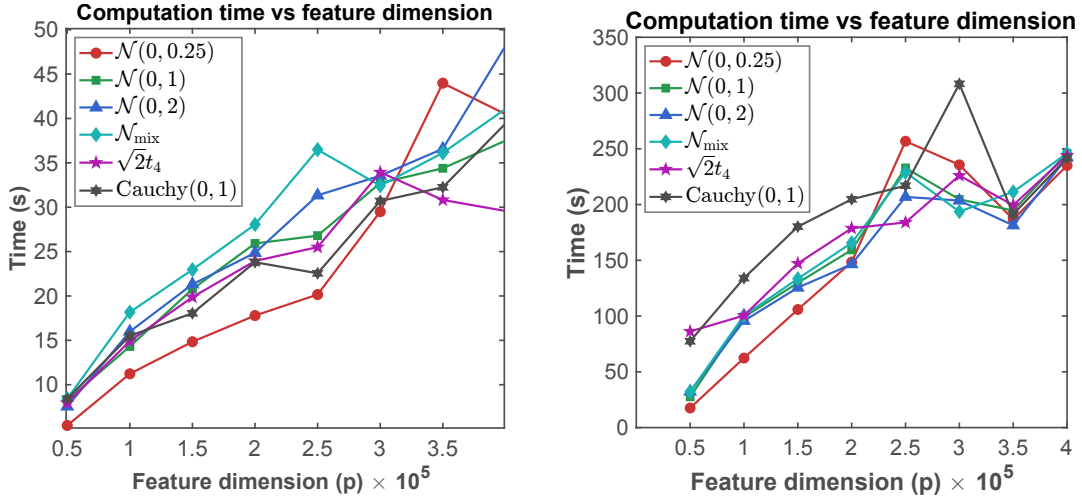


Figure 1: PALM computation time vs. dimension p for fixed $n = 500$ (left) and $n = 2000$ (right).

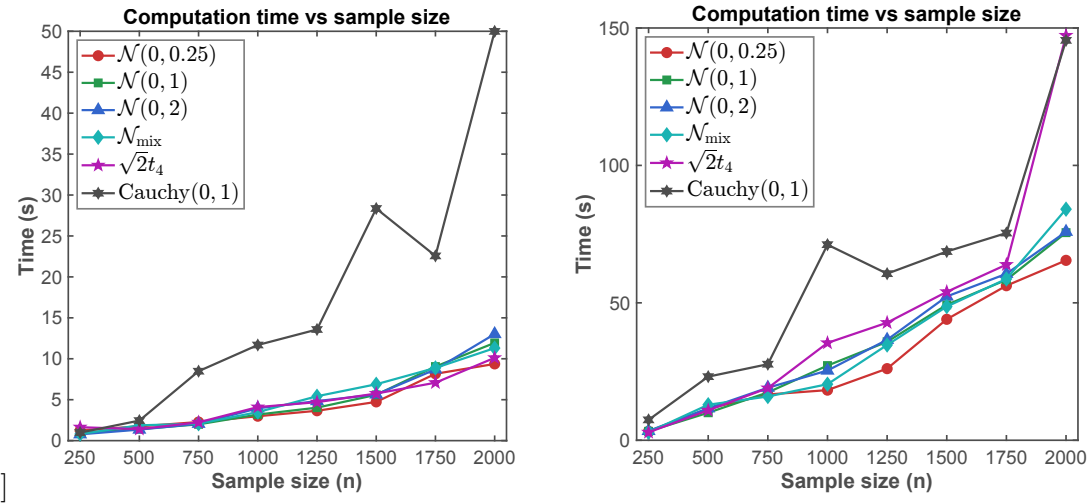


Figure 2: PALM computation time vs. sample size n at fixed dimensions $p = 8000$ (left) and $p = 100000$ (right).

complexity in the dimension p and moderate growth with respect to the sample size n . This makes it a powerful tool for tackling large-scale group-sparse regression problems.

4.4 Benchmarking PALM on ℓ_1 -Regularized Rank Regression

Note that if we set $\Psi(\beta) = \|\beta\|_1$ in (3), the model reduces to rank regression with lasso regularization. In other words, our proposed algorithm can directly solve the ℓ_1 -regularized rank regression problem. This subsection evaluates the computational efficiency of our method in this setting. For comparison, we benchmark against the state-of-the-art Proximal–Proximal Majorization–Minimization (PPMM) algorithm of [Tang et al. \[2023\]](#), which was originally designed for rank regression with difference-of-convex penalties. Specifically, the ℓ_1 -regularized case corresponds to Step 1 of Algorithm 3 in [Tang et al. \[2023\]](#), which, as noted in the introduction, employs a computationally intensive triple-loop architecture.

Data Generation. To evaluate the performance of our algorithm for rank regression with lasso regularization, we largely follow the data generation framework described in Section 4.2 on group lasso regularized rank regression. The noise distributions remain the same (settings E1–E6). For the covariates, we introduce an additional design (C3) from [Tang et al. \[2023\]](#) to facilitate direct comparison with PPMM. For the coefficients, we add elementwise-sparse designs (S3)–(S4) to match the ℓ_1 setting. The rows of the design matrix X are sampled i.i.d. from the p -dimensional multivariate Gaussian distribution $\mathcal{N}(0, \Sigma)$ with

(C3) Equi-correlation: $\Sigma_{ij} = 0.5$ for all $i \neq j$, and $\Sigma_{ii} = 1$.

The true coefficient vector $\beta^* \in \mathbb{R}^p$ exhibits elementwise sparsity with:

(S3) Sparse signal: $\beta^* = (\underbrace{\sqrt{3}, \dots, \sqrt{3}}_{k \text{ entries}}, 0, \dots, 0)^\top$, $k = \begin{cases} 3 & \text{if } p \leq 8000, \\ \lfloor 0.001p \rfloor & \text{if } p > 8000. \end{cases}$

(S4) Decaying signal: $\beta^* = (\underbrace{2, \dots, 2}_{4m}, \underbrace{1.75, \dots, 1.75}_{3m}, \underbrace{0.25, \dots, 0.25}_{3m}, 0, \dots, 0)^\top$, where the scaling factor m is taken as $m = \begin{cases} 1 & \text{if } p \leq 8000, \\ \lceil p/2500 \rceil & \text{if } p > 8000. \end{cases}$

To access solution quality, we report both the KKT residual η_{kkt} defined in (29) and the relative duality gap defined as

$$\text{relgap} := \frac{|\text{pobj} - \text{dobj}|}{1 + |\text{pobj}| + |\text{dobj}|},$$

where

$$\text{pobj} := L(X\beta - y) + \lambda\Psi(\beta) \quad \text{and} \quad \text{dobj} := -\langle y, w \rangle - L^*(w) - \lambda\Psi^*(-\lambda^{-1}X^\top w)$$

are the primal and dual objective values, respectively. It is worth noting that the implementation of PPMM is not publicly available. We therefore reproduced the algorithm based on the description in [Tang et al. \[2023\]](#). As shown in Table 5, which corresponds exactly to the setting reported in [Tang et al. \[2023\]](#), our implementation of PPMM achieves running times that are significantly faster than those reported in the original paper. This marked improvement not only confirms the validity of our reproduction but also establishes a strong baseline for fair comparisons.

Table 5 first reports results under the same experimental setting as in [Tang et al. \[2023\]](#). We observe that PALM consistently runs faster than PPMM while attaining comparable accuracy.

Table 5: Comparison of PALM and PPMM for solving ℓ_1 -regularized rank regression with 2000×8000 design matrix under covariance structure (C3), evaluated across different signal patterns (S3)–(S4) and error distributions (E1)–(E6)

| Signal Pattern | Noise | λ | Time | | η_{kkt} | | relgap | |
|----------------|----------------------------|-----------|-------|-------|---------------------|---------|---------|----------|
| | | | PALM | PPMM | PALM | PPMM | PALM | PPMM |
| (S3) | $\mathcal{N}(0, 0.25)$ | 0.104 | 00:04 | 00:17 | 9.84e-7 | 9.83e-7 | 2.27e-8 | 5.02e-10 |
| | $\mathcal{N}(0, 1)$ | 0.102 | 00:04 | 00:13 | 9.90e-7 | 8.74e-7 | 5.94e-8 | 9.23e-10 |
| | $\mathcal{N}(0, 2)$ | 0.102 | 00:04 | 00:10 | 9.73e-7 | 9.88e-7 | 9.05e-8 | 9.21e-9 |
| | \mathcal{N}_{mix} | 0.100 | 00:04 | 00:14 | 9.75e-7 | 9.94e-7 | 3.44e-7 | 1.27e-9 |
| | $\sqrt{2}t_4$ | 0.101 | 00:04 | 00:15 | 9.54e-7 | 9.23e-7 | 6.34e-8 | 4.47e-9 |
| | Cauchy(0, 1) | 0.103 | 00:11 | 00:13 | 9.37e-7 | 4.98e-7 | 1.27e-6 | 5.48e-8 |
| (S4) | $\mathcal{N}(0, 0.25)$ | 0.105 | 00:07 | 00:28 | 9.99e-7 | 9.20e-7 | 2.38e-9 | 3.17e-9 |
| | $\mathcal{N}(0, 1)$ | 0.103 | 00:07 | 00:25 | 9.78e-7 | 8.89e-7 | 8.66e-9 | 1.51e-9 |
| | $\mathcal{N}(0, 2)$ | 0.102 | 00:09 | 00:29 | 9.78e-7 | 9.10e-7 | 2.39e-8 | 2.57e-9 |
| | \mathcal{N}_{mix} | 0.100 | 00:12 | 00:31 | 9.44e-7 | 8.98e-7 | 3.56e-8 | 3.43e-9 |
| | $\sqrt{2}t_4$ | 0.100 | 00:09 | 00:26 | 9.52e-7 | 8.24e-7 | 7.34e-9 | 1.78e-8 |
| | Cauchy(0, 1) | 0.103 | 00:21 | 00:25 | 7.28e-7 | 7.20e-7 | 2.96e-7 | 8.45e-8 |

Across both signal patterns and all noise types, PALM completes the tasks in seconds (ranging from 4 to 21 seconds), while PPMM requires substantially longer runtimes (ranging from 10 to 31 seconds). This represents a significant speedup, with PALM often finishing in half the time of PPMM or even less. Under the more complex signal pattern (S4), which is less sparse than (S3), both algorithms require longer computation time, as expected. Despite the increased problem difficulty, PALM maintains a clear efficiency advantage. These results confirm the practical efficiency of PALM under the same settings used in prior work, while ensuring a fair and reproducible comparison.

We then proceed to test more challenging large-scale problems under varying distribution of covariates, signal patterns, and error distributions, with results summarized in Tables 6 and 7. The results reveal that PALM maintains a decisive and robust efficiency advantage as the problem size grows. Under the (C2)–(S3) setting (Table 6), when the dimension expands from (2000, 20000) to the more challenging (4000, 40000), the runtime of PALM increases gracefully from seconds to under half a minute for most noise types. In contrast, PPMM’s runtime escalates sharply from less one minute to over 4 minutes, representing an order-of-magnitude slower scaling. This efficiency gap is further amplified under the denser signal pattern (S4) in Table 7. For the largest problem (4000, 40000), PALM robustly obtains a solution within 6–8 minutes across all noise distributions, while PPMM’s runtime varies widely from 35 to 60 minutes, highlighting its sensitivity to problem difficulty. Despite these substantial differences in computational time, both algorithms consistently achieve high-quality solutions with η_{kkt} below 10^{-6} , underscoring PALM’s superior scalability without compromising accuracy.

Finally, we evaluate both algorithms on real-world datasets from the KEEL repository [Alcalá-Fdez et al., 2011]. Following Tang et al. [2023], the features of each dataset are expanded into a higher-dimensional space using polynomial basis functions to create high-dimensional settings for scalability evaluation. The order of expansion is encoded in the dataset name: for example,

Table 6: Comparison of PALM and PPMM for solving ℓ_1 -regularized rank regression with design matrix X under covariance structure (C2) and signal pattern (S3), evaluated across varying problem dimensions and error distributions (E1)–(E6)

| Noise | Dimension | λ | Time | | η_{kkt} | | relgap | |
|------------------------|---------------|-----------|-------|-------|---------------------|---------|---------|----------|
| | | | PALM | PPMM | PALM | PPMM | PALM | PPMM |
| $\mathcal{N}(0, 0.25)$ | (2000, 20000) | 0.116 | 00:06 | 00:50 | 6.54e-7 | 3.70e-7 | 1.17e-7 | 1.12e-11 |
| | (2000, 40000) | 0.119 | 00:13 | 01:22 | 3.72e-7 | 4.27e-7 | 4.48e-9 | 5.32e-10 |
| | (4000, 40000) | 0.085 | 00:26 | 04:02 | 4.48e-7 | 1.32e-7 | 1.87e-7 | 5.79e-8 |
| $\mathcal{N}(0, 1)$ | (2000, 20000) | 0.117 | 00:05 | 00:35 | 6.04e-7 | 5.96e-7 | 1.29e-7 | 1.35e-9 |
| | (2000, 40000) | 0.121 | 00:11 | 01:09 | 5.26e-7 | 4.38e-7 | 9.76e-9 | 6.23e-9 |
| | (4000, 40000) | 0.086 | 00:17 | 03:54 | 5.42e-7 | 1.59e-7 | 4.45e-8 | 3.63e-7 |
| $\mathcal{N}(0, 2)$ | (2000, 20000) | 0.117 | 00:06 | 00:40 | 8.76e-7 | 5.99e-7 | 3.32e-7 | 4.47e-7 |
| | (2000, 40000) | 0.122 | 00:13 | 01:12 | 5.87e-7 | 5.45e-7 | 4.28e-8 | 2.46e-8 |
| | (4000, 40000) | 0.085 | 00:17 | 02:58 | 2.64e-7 | 1.92e-7 | 5.96e-8 | 6.39e-7 |
| N_{mix} | (2000, 20000) | 0.116 | 00:04 | 00:32 | 8.96e-7 | 6.57e-7 | 2.11e-7 | 1.59e-8 |
| | (2000, 40000) | 0.121 | 00:08 | 01:05 | 9.19e-7 | 4.59e-7 | 2.21e-8 | 3.97e-9 |
| | (4000, 40000) | 0.085 | 00:17 | 03:05 | 9.12e-7 | 1.10e-7 | 6.26e-8 | 1.74e-7 |
| $\sqrt{2}t_4$ | (2000, 20000) | 0.116 | 00:05 | 00:34 | 7.52e-7 | 5.99e-7 | 2.65e-7 | 6.79e-8 |
| | (2000, 40000) | 0.121 | 00:07 | 00:54 | 8.34e-7 | 4.58e-7 | 2.72e-7 | 4.63e-9 |
| | (4000, 40000) | 0.085 | 00:16 | 03:16 | 3.08e-7 | 1.17e-7 | 4.05e-8 | 1.22e-7 |
| Cauchy(0, 1) | (2000, 20000) | 0.118 | 00:06 | 00:36 | 8.49e-7 | 5.15e-7 | 1.82e-6 | 1.59e-7 |
| | (2000, 40000) | 0.121 | 00:12 | 01:07 | 4.75e-7 | 3.10e-7 | 6.29e-8 | 1.69e-8 |
| | (4000, 40000) | 0.085 | 00:20 | 03:40 | 2.70e-7 | 5.59e-7 | 9.08e-7 | 1.18e-5 |

Table 7: Comparison of PALM and PPMM for solving ℓ_1 -regularized rank regression with design matrix X under covariance structure (C3) and signal pattern (S4), evaluated across varying problem dimensions and error distributions (E1)–(E6)

| Noise | Dimension | λ | Time | | η_{kkt} | | relgap | |
|------------------------|---------------|-----------|-------|-------|---------------------|---------|---------|----------|
| | | | PALM | PPMM | PALM | PPMM | PALM | PPMM |
| $\mathcal{N}(0, 0.25)$ | (2000, 20000) | 0.106 | 01:11 | 02:57 | 9.13e-7 | 4.84e-7 | 1.10e-8 | 8.42e-10 |
| | (2000, 40000) | 0.108 | 01:52 | 05:21 | 7.51e-7 | 9.11e-7 | 2.35e-6 | 2.87e-6 |
| | (4000, 40000) | 0.075 | 07:07 | 36:27 | 4.81e-7 | 3.39e-8 | 2.28e-8 | 1.67e-8 |
| $\mathcal{N}(0, 1)$ | (2000, 20000) | 0.103 | 01:18 | 02:20 | 9.70e-7 | 4.98e-7 | 1.11e-9 | 6.48e-8 |
| | (2000, 40000) | 0.110 | 01:52 | 04:53 | 9.30e-7 | 9.53e-7 | 2.78e-6 | 2.79e-6 |
| | (4000, 40000) | 0.077 | 07:52 | 34:58 | 7.28e-7 | 6.02e-7 | 3.23e-8 | 2.10e-6 |
| $\mathcal{N}(0, 2)$ | (2000, 20000) | 0.105 | 01:18 | 02:11 | 5.36e-7 | 4.40e-7 | 1.65e-8 | 4.67e-7 |
| | (2000, 40000) | 0.111 | 01:53 | 04:38 | 9.44e-7 | 8.60e-7 | 2.54e-6 | 2.53e-6 |
| | (4000, 40000) | 0.078 | 07:43 | 59:14 | 3.40e-7 | 2.13e-7 | 5.73e-9 | 6.87e-7 |
| N_{mix} | (2000, 20000) | 0.105 | 01:06 | 02:11 | 7.59e-7 | 4.99e-7 | 5.01e-8 | 1.61e-8 |
| | (2000, 40000) | 0.108 | 01:23 | 04:12 | 9.55e-7 | 8.65e-7 | 2.33e-6 | 2.40e-6 |
| | (4000, 40000) | 0.077 | 06:39 | 40:04 | 5.41e-7 | 2.47e-7 | 1.20e-7 | 2.07e-6 |
| $\sqrt{2}t_4$ | (2000, 20000) | 0.106 | 01:01 | 01:57 | 7.54e-7 | 5.49e-7 | 2.83e-8 | 2.33e-7 |
| | (2000, 40000) | 0.108 | 01:24 | 04:36 | 8.23e-7 | 8.52e-7 | 1.98e-6 | 2.50e-6 |
| | (4000, 40000) | 0.078 | 06:55 | 37:47 | 3.64e-7 | 5.55e-8 | 6.56e-9 | 2.54e-7 |
| Cauchy(0, 1) | (2000, 20000) | 0.108 | 01:05 | 02:00 | 5.47e-7 | 6.91e-7 | 1.36e-7 | 2.18e-5 |
| | (2000, 40000) | 0.107 | 01:25 | 03:37 | 3.15e-7 | 8.14e-7 | 8.63e-7 | 9.56e-7 |
| | (4000, 40000) | 0.076 | 06:51 | 47:55 | 5.12e-7 | 1.40e-7 | 2.02e-7 | 1.06e-5 |

“baseball5” denotes a fifth-order expansion. The comparative results are presented in Table 8. As shown, both algorithms successfully solve all instances to high accuracy. PALM demonstrates

Table 8: Comparison of PALM and PPMM for solving ℓ_1 -regularized rank regression on real datasets

| Data | Dimension | λ | Time | | η_{kkt} | | relgap | |
|-----------------|---------------|-----------|-------|-------|---------------------|---------|---------|----------|
| | | | PALM | PPMM | PALM | PPMM | PALM | PPMM |
| baseball5 | (337, 17067) | 2.1e-1 | 00:04 | 00:14 | 6.12e-7 | 3.85e-7 | 7.84e-7 | 3.32e-5 |
| compactiv51tra4 | (6553, 12649) | 5.4e-2 | 00:54 | 30:34 | 3.69e-7 | 7.51e-7 | 8.96e-7 | 7.22e-1 |
| concrete7 | (1030, 6434) | 1.2e-1 | 00:03 | 00:09 | 9.76e-7 | 7.74e-7 | 4.67e-7 | 2.10e-8 |
| dee10 | (365, 8007) | 1.9e-1 | 00:02 | 00:05 | 9.26e-7 | 9.77e-7 | 3.05e-8 | 2.22e-7 |
| friedman10 | (1200, 3002) | 1.1e-1 | 00:01 | 00:07 | 8.78e-7 | 1.00e-6 | 3.27e-7 | 9.89e-8 |
| puma32h51tst3 | (1639, 6544) | 1.2e-1 | 00:04 | 04:43 | 5.99e-7 | 9.14e-7 | 4.28e-9 | 3.05e-11 |
| wizmir7 | (1461, 11439) | 9.2e-2 | 00:03 | 00:27 | 9.78e-7 | 5.09e-7 | 2.08e-8 | 1.14e-7 |

significantly superior computational efficiency across all datasets. A particularly striking example is the “compactiv51tra4” dataset, where PALM converges in under one minute, while PPMM requires over 30 minutes, representing a speedup of more than 30 times. Similarly, on the “puma32h51tst3” dataset, PALM solves the problem in just 4 seconds compared to PPMM’s nearly 5 minutes. Even on smaller datasets, PALM maintains a consistent 2- to 7-fold advantage. This strong speed advantage highlights the practical strength and scalability of the PALM algorithm when applied to real-data problems.

5 Conclusion

This paper proposed a group lasso regularized Wilcoxon rank regression estimator for robust high-dimensional regression with grouped coefficients, together with a data-driven, simulation-based rule for selecting the regularization parameter. We established the finite-sample error bound for the estimator, with a theoretical framework that extends beyond group regularization to general norm-based penalties under mild structural conditions. To address the associated optimization problem, we developed a superlinearly convergent proximal augmented Lagrangian method (PALM), where subproblems are efficiently solved by a semismooth Newton method. Numerical experiments demonstrate that the proposed estimator attains superior estimation accuracy and reliable group selection in various data-generating settings, while the PALM algorithm exhibits strong scalability and consistently outperforms state-of-the-art alternatives on synthetic and real data.

A Proofs of supporting lemmas and additional results

This section presents the proofs of the supporting lemmas in Section 2.3, along with an additional lemma used in the analysis.

of Lemma 2. Denote $\hat{\gamma} = \hat{\gamma}(\lambda^*)$. By the equivalence between the solutions of (3) and (5) under the transformation $\beta = \gamma + \beta^*$, we have $\hat{\gamma} = \arg \min_{\gamma \in \mathbb{R}^p} F_{\lambda^*}(\gamma)$, where $F_{\lambda^*}(\cdot)$ is defined in (5). Then

$F_{\lambda^*}(\hat{\gamma}) \leq F_{\lambda^*}(0)$, which implies

$$\begin{aligned} L_0(\hat{\gamma}) - L_0(0) &\leq \lambda^* \left(\Psi(\beta^*) - \Psi(\hat{\beta}(\lambda^*)) \right) \\ &\leq \lambda^* \Psi_\Omega(\beta^*) - \lambda^* \Psi_\Omega(\hat{\beta}(\lambda^*)) - \lambda^* \Psi_{\bar{\Omega}}(\hat{\beta}(\lambda^*)) \leq \lambda^* \Psi_\Omega(\hat{\gamma}) - \lambda^* \Psi_{\bar{\Omega}}(\hat{\gamma}), \end{aligned} \quad (\text{A1})$$

where the second inequality follows from the decomposition (10), and the last equality follows from the triangle inequality and the fact that $\Psi_{\bar{\Omega}}(\beta^*) = 0$. On the other hand, by the convexity of $L_0(\cdot)$, we have

$$L_0(\hat{\gamma}) - L_0(0) \geq \langle \hat{\gamma}, S_n \rangle \geq -\Psi(\hat{\gamma}) \cdot \Psi^d(S_n),$$

where S_n in (7) is the subgradient of $L_0(\gamma)$ at 0. The choice of λ^* in (8) implies $\text{pr}(\lambda^* \geq c_0 \Psi^d(S_n)) = 1 - \alpha_0$, which means

$$L_0(\hat{\gamma}) - L_0(0) \geq -\frac{\lambda^*}{c_0} \Psi(\hat{\gamma}) \geq -\frac{\lambda^*}{c_0} (\Psi_\Omega(\hat{\gamma}) + \Psi_{\bar{\Omega}}(\hat{\gamma})) \quad (\text{A2})$$

holds with probability $1 - \alpha_0$. Combining (A1) and (A2), we can see that

$$\text{pr} \left(\Psi_{\bar{\Omega}}(\hat{\gamma}) \leq \frac{c_0 + 1}{c_0 - 1} \Psi_\Omega(\hat{\gamma}) \right) = 1 - \alpha_0,$$

which completes the proof. \square

of Lemma 3. By writing $S_n = (s_1, \dots, s_p)^\top$, we have

$$s_k = \frac{1}{n(n-1)} \sum_{i=1}^n \sum_{j \neq i} (X_{jk} - X_{ik}) \text{ sign}(\epsilon_i - \epsilon_j), \quad k \in [p].$$

For any $t > 0$. The concentration inequality for U-statistics [Wang et al., 2020, Lemma A] together with Assumption (A-1) implies that $\text{pr}(|s_k| \geq t/c_p) \leq 2 \exp(-nt^2/(32b_1^2 c_p^2))$. Then we have that

$$\text{pr} \left(\Psi^d(S_n) \geq t \right) \leq \text{pr} \left(\|S_n\|_\infty \geq \frac{t}{c_p} \right) \leq \sum_{k=1}^p \text{pr} \left(|s_k| \geq \frac{t}{c_p} \right) \leq 2p \exp \left(-\frac{nt^2}{32b_1^2 c_p^2} \right),$$

where the first and second inequalities follow from (11) and the union bound, respectively. \square

We next provide a technical lemma that is used in the proof of Theorem 1 in Section 2.3.

Lemma 4. *Given a convex function $g : \mathbb{R}^p \rightarrow \mathbb{R}$, a cone Γ in \mathbb{R}^p , and any $\delta > 0$. Suppose $\inf_{y \in \Gamma} \{g(y) \mid \|y\|_2 = \delta\} > g(0)$, then we have $\inf_{y \in \Gamma} \{g(y) \mid \|y\|_2 > \delta\} > g(0)$.*

Proof. For any $y \in \Gamma$ satisfying $\|y\|_2 > \delta$. Since Γ is a cone, we have $(\delta/\|y\|_2)y \in \Gamma$. By the convexity of $g(\cdot)$, we have $(1 - \delta/\|y\|_2)g(0) + (\delta/\|y\|_2)g(y) \geq g((\delta/\|y\|_2)y)$. Rearranging this inequality, we obtain

$$\frac{\delta}{\|y\|_2} (g(y) - g(0)) \geq g \left(\frac{\delta}{\|y\|_2} y \right) - g(0) \geq \inf_{x \in \Gamma} \{g(x) \mid \|x\|_2 = \delta\} - g(0) > 0,$$

which indicates $g(y) - g(0) > 0$. This further implies that

$$g(y) - g(0) \geq \frac{\delta}{\|y\|_2} (g(y) - g(0)) \geq \inf_{x \in \Gamma} \{g(x) \mid \|x\|_2 = \delta\} - g(0) > 0.$$

By taking the infimum of y over all $y \in \Gamma$ with $\|y\|_2 > \delta$, we have

$$\inf_{x \in \Gamma} \{g(x) \mid \|x\|_2 > \delta\} - g(0) \geq \inf_{x \in \Gamma} \{g(x) \mid \|x\|_2 = \delta\} - g(0) > 0,$$

and the conclusion follows. \square

References

Jesús Alcalá-Fdez, Alberto Fernández, Julián Luengo, Joaquín Derrac, and Salvador García. KEEL data-mining software tool: Data set repository, integration of algorithms and experimental analysis framework. *Journal of Multiple-Valued Logic and Soft Computing*, 17:255–287, 2011. URL <https://api.semanticscholar.org/CorpusID:262474338>.

Albert E. Beaton and John W. Tukey. The fitting of power series, meaning polynomials, illustrated on band-spectroscopic data. *Technometrics*, 16(2):147–185, 1974. doi: 10.1080/00401706.1974.10489171. URL <https://www.tandfonline.com/doi/abs/10.1080/00401706.1974.10489171>.

Michael J. Best and Nilotpal Chakravarti. Active set algorithms for isotonic regression; a unifying framework. *Mathematical Programming*, 47(1):425–439, 05 1990. ISSN 1436-4646. doi: 10.1007/BF01580873. URL <https://doi.org/10.1007/BF01580873>.

Peter J. Bickel, Ya'acov Ritov, and Alexandre B. Tsybakov. Simultaneous analysis of Lasso and Dantzig selector. *The Annals of Statistics*, 37(4):1705–1732, 2009. ISSN 00905364, 21688966. URL <http://www.jstor.org/stable/30243685>.

Peter Bühlmann and Sara Van De Geer. *Statistics for High-Dimensional Data: Methods, Theory and Applications*. Springer Berlin Heidelberg, 2011. ISBN 9783642201929. doi: 10.1007/978-3-642-20192-9. URL <http://dx.doi.org/10.1007/978-3-642-20192-9>.

Anders Eklund, Thomas E. Nichols, and Hans Knutsson. Cluster failure: Why fMRI inferences for spatial extent have inflated false-positive rates. *Proceedings of the National Academy of Sciences*, 113(28):7900–7905, 2016. doi: 10.1073/pnas.1602413113.

Jianqing Fan, Quefeng Li, and Yuyan Wang. Estimation of high dimensional mean regression in the absence of symmetry and light tail assumptions. *Journal of the Royal Statistical Society Series B: Statistical Methodology*, 79(1):247–265, 2016. doi: 10.1111/rssb.12166.

Jianqing Fan, Cong Ma, and Kaizheng Wang. Comment on “a tuning-free robust and efficient approach to high-dimensional regression”. *Journal of the American Statistical Association*, 115(532):1720–1725, 2020. doi: 10.1080/01621459.2020.1837138. URL <https://doi.org/10.1080/01621459.2020.1837138>.

Thomas P. Hettmansperger and Joseph W. McKean. *Robust Nonparametric Statistical Methods*. CRC Press, Boca Raton, 2nd edition, 2010. ISBN 978-1-4200-7366-6. doi: 10.1201/b10451.

Peter J Huber. Robust regression: Asymptotics, conjectures and Monte Carlo. *The Annals of Statistics*, 1(5):799–821, 1973.

Peter J. Huber. Robust statistics. In Miodrag Lovric, editor, *International Encyclopedia of Statistical Science*, pages 1248–1251. Springer Berlin Heidelberg, 2011. ISBN 978-3-642-04898-2. doi: 10.1007/978-3-642-04898-2_594.

Louis A. Jaeckel. Estimating regression coefficients by minimizing the dispersion of the residuals. *The Annals of Mathematical Statistics*, 43(5):1449–1458, 1972. doi: 10.1214/aoms/1177692377. URL <https://doi.org/10.1214/aoms/1177692377>.

Nikola Janjušević, Amirhossein Khalilian-Gourtani, Adeen Flinker, Li Feng, and Yao Wang. GroupCDL: Interpretable denoising and compressed sensing MRI via learned group-sparsity and circulant attention. *IEEE Transactions on Computational Imaging*, 11:201–212, 2025. doi: 10.1109/TCI.2025.3539021.

Jana Jurečková and Pranab K. Sen. *Robust Statistical Procedures: Asymptotics and Interrelations*. Wiley Series in Probability and Statistics. John Wiley & Sons, 1996. ISBN 978-0-471-55553-8. doi: 10.1002/9780470316950. URL <https://doi.org/10.1002/9780470316950>.

Roger Koenker. *Quantile Regression*. Econometric Society Monographs. Cambridge University Press, 2005.

Roger Koenker and Gilbert Bassett. Regression quantiles. *Econometrica*, 46(1):33–50, 1978. ISSN 00129682, 14680262. URL <http://www.jstor.org/stable/1913643>.

Michel Ledoux and Michel Talagrand. *Probability in Banach Spaces*. Springer Berlin Heidelberg, 1991. ISBN 9783642202124. doi: 10.1007/978-3-642-20212-4. URL <http://dx.doi.org/10.1007/978-3-642-20212-4>.

Xudong Li, Defeng Sun, and Kim-Chuan Toh. On efficiently solving the subproblems of a level-set method for fused Lasso problems. *SIAM Journal on Optimization*, 28(2):1842–1866, 2018. doi: 10.1137/17M1136390. URL <https://doi.org/10.1137/17M1136390>.

Xudong Li, Defeng Sun, and Kim-Chuan Toh. An asymptotically superlinearly convergent semismooth Newton augmented Lagrangian method for linear programming. *SIAM Journal on Optimization*, 30(3):2410–2440, 2020.

Meixia Lin, Yong-Jin Liu, Defeng Sun, and Kim-Chuan Toh. Efficient sparse semismooth Newton methods for the clustered Lasso problem. *SIAM Journal on Optimization*, 29(3):2026–2052, 2019.

Xiaotong Lu, Weisheng Dong, Zhenxuan Fang, Jie Lin, Xin Li, and Guangming Shi. Growing-before-pruning: A progressive neural architecture search strategy via group sparsity and deterministic annealing. *Pattern Recognition*, 166:111697, 2025. doi: 10.1016/j.patcog.2025.111697.

Colin McDiarmid. On the method of bounded differences. In J. Siemons, editor, *Surveys in Combinatorics, 1989: Invited Papers at the Twelfth British Combinatorial Conference*, volume 141 of *London Mathematical Society Lecture Note Series*, pages 148–188. Cambridge University Press, Cambridge, 1989. doi: 10.1017/cbo9781107359949.008. URL <http://dx.doi.org/10.1017/cbo9781107359949.008>.

J.J. Moreau. Proximité et dualité dans un espace hilbertien. *Bulletin de la Société Mathématique de France*, 93:273–299, 1965. doi: 10.24033/bsmf.1625. URL <https://www.numdam.org/articles/10.24033/bsmf.1625/>.

Sahand N. Negahban, Pradeep Ravikumar, Martin J. Wainwright, and Bin Yu. A unified framework for high-dimensional analysis of M-estimators with decomposable regularizers. *Statistical Science*, 27(4):538–557, 2012. doi: 10.1214/12-STS400. URL <https://doi.org/10.1214/12-STS400>.

Jorge Nocedal and Stephen J. Wright. *Numerical Optimization*. Springer Series in Operations Research and Financial Engineering. Springer, New York, NY, 2 edition, July 2006. ISBN 978-0-387-30303-1. doi: 10.1007/978-0-387-40065-5. URL <https://doi.org/10.1007/978-0-387-40065-5>.

Sumitra Purkayastha. Simple proofs of two results on convolutions of unimodal distributions. *Statistics & Probability Letters*, 39(2):97–100, 1998. ISSN 0167-7152. doi: [https://doi.org/10.1016/S0167-7152\(98\)00013-3](https://doi.org/10.1016/S0167-7152(98)00013-3). URL <https://www.sciencedirect.com/science/article/pii/S0167715298000133>.

Stephen M Robinson. Some continuity properties of polyhedral multifunctions. In *Mathematical Programming at Oberwolfach*, pages 206–214. Springer, 2009.

R. Tyrrell Rockafellar. Monotone operators and the proximal point algorithm. *SIAM Journal on Control and Optimization*, 14(5):877–898, 1976a. doi: 10.1137/0314056. URL <https://doi.org/10.1137/0314056>.

R. Tyrrell Rockafellar. Augmented Lagrangians and applications of the proximal point algorithm in convex programming. *Mathematics of Operations Research*, 1(2):97–116, 1976b. doi: 10.1287/moor.1.2.97. URL <https://doi.org/10.1287/moor.1.2.97>.

R. Tyrrell Rockafellar and Roger J.-B. Wets. *Variational Analysis*. Grundlehren der mathematischen Wissenschaften. Springer, New York, 3rd edition, 2009. ISBN 978-3-540-62772-2. doi: 10.1007/978-3-540-62772-2. Corrected 3rd printing.

Qiang Sun, Wen-Xin Zhou, and Jianqing Fan. Adaptive Huber regression. *Journal of the American Statistical Association*, 115(529):254–265, 2020.

Peipei Tang, Chengjing Wang, and Bo Jiang. A proximal-proximal majorization-minimization algorithm for nonconvex rank regression problems. *IEEE Transactions on Signal Processing*, 2023.

Lan Wang, Bo Peng, and Runze Li. A high-dimensional nonparametric multivariate test for mean vector. *Journal of the American Statistical Association*, 110(512):1658–1669, 2015. doi: 10.1080/01621459.2014.988215. PMID: 26848205.

Lan Wang, Bo Peng, Jelena Bradic, Runze Li, and Yunan Wu. A tuning-free robust and efficient approach to high-dimensional regression. *Journal of the American Statistical Association*, 115(532):1700–1714, October 2020. ISSN 1537-274X. doi: 10.1080/01621459.2020.1840989. URL <http://dx.doi.org/10.1080/01621459.2020.1840989>.

Ming Yuan and Yi Lin. Model selection and estimation in regression with grouped variables. *Journal of the Royal Statistical Society Series B: Statistical Methodology*, 68(1):49–67, 2006. doi: 10.1111/j.1467-9868.2005.00532.x.

Yangjing Zhang, Ning Zhang, Defeng Sun, and Kim-Chuan Toh. An efficient Hessian based algorithm for solving large-scale sparse group Lasso problems. *Mathematical Programming*, 179(1):223–263, 2020. doi: 10.1007/s10107-018-1329-6.

Xin-Yuan Zhao, Defeng Sun, and Kim-Chuan Toh. A Newton-CG augmented Lagrangian method for semidefinite programming. *SIAM Journal on Optimization*, 20(4):1737–1765, 2010.